Variations in biomass, production, and respiration of fine roots in a young larch forest

（カラマツ若齢林における細根のバイオマス，生産量および呼吸の変動）

Hokkaido University Graduate School of Agriculture

Frontiers in Environment Sciences　Doctor Course

Cui Rui

Abstract

Soil respiration (R_s) accounts for 30–80% of total respiration in forest ecosystems, indicating R_s plays a crucial role in terrestrial carbon cycles. The R_s is composed of root respiration (R_r) and microbial heterotrophic respiration (R_h). Plant roots are different in metabolism and functions according to size and order. Fine roots (typically < 2 mm in diameter) perform important functions and govern belowground carbon cycles. However, the phenological variation of the functions is not well understood. Thus, we adopted an approach to partition R_r into respirations for growth (R_g), maintenance (R_m), and ion uptake (R_{ion}) using modified empirical models. We conducted field experiments on R_s and fine root dynamics, and transpiration in a larch-dominated young forest on the bare ground after removing surface organic soil to parameterize the models.

The field experiments were conducted in 2017–2018 (E1) and 2019–2020 (E2) in a regenerating forest dominated by Japanese larch in Tomakomai, Hokkaido. The top organic soil was removed after typhoon disturbance in 2004. Collar pairs consisting of control (CC) and trenched (TC) ones were installed at 0.5 m (N) and 1 m (F) from isolated larch trees (n = 10 (E1) and 18 (E2)). Soil CO_2 fluxes (R_{CC} and R_{TC}) were periodically measured on the collars by a chamber method. The R_{CC} and R_{TC} were continuously estimated throughout the experimental periods from soil temperature (T_s) using exponential equations. CO_2 efflux through dead root decomposition (R_{DR}) in trenched collars was also estimated. The R_h was calculated as $R_{TC} - R_{DR}$, and R_r was derived as $R_{CC} - R_h$. Fine root biomass (B_f, g DM m^{-2}) and production (P_f, g DM m^{-2} d^{-1}) were periodically measured in CC by the sequential coring and ingrowth core methods, respectively. In addition, sap flow was measured by a thermal dispersion method only in E2. The following two models were applied to partition R_r (g C m^{-2} d^{-1}):

$$R_r = R_m + R_g = c_1 \cdot P_f + d_1 \cdot exp(f_1 \cdot T_s) \cdot (B_f + B_c) \quad (1)$$

$$R_r = R_m + R_g + R_{ion} = c_2 \cdot P_f + d_2 \cdot exp(f_2 \cdot T_s) \cdot (B_f + B_c) + g \cdot T_r \cdot B_f \quad (2)$$

where c, d, f, and g are fitting parameters, B_c coarse root biomass (g DM m^{-2}), and T_r transpiration per fine root biomass (g H_2O g DM^{-1} d^{-1}).

Annual R_s was 493 ± 45 (N) and 311 ± 34 g C m^{-2} yr^{-1} (F) (mean ± standard error) in E1, and R_r accounted for 37% (N) and 16% (F) of R_s. Despite no seasonal variation in B_f, P_f decreased in the cold season. Annual P_f was 81 ± 22 (N) and 41 ± 10 g DM m^{-2} yr^{-1} (F), and

annual mean B_f was 70 ± 9 (N) and 13 ± 3 g DM m^{-2} yr^{-1} (F). Model 1 (M1) was significantly parameterized (r^2 = 0.59, p < 0.001) using the field data (n = 50). Annual R_r was estimated to be 107 g C m^{-2} yr^{-1} and accounted for 25% of R_s. The R_r was partitioned into fine root R_g, fine root R_m, and coarse root R_m by 30, 44 and 26%, respectively. In E2, annual R_s was 610 ± 26 (N) and 474 ± 52 g C m^{-2} yr^{-1} (F), and R_r accounted for 47% and 45% of R_s, respectively. The B_f increased slightly in the growing season, whereas P_f clearly decreased in the cold season and peaked in July. Annual P_f was 115 ± 7 (N) and 102 ± 10 g DM m^{-2} yr^{-1} (F), and mean B_f was 133 ± 13 (N) and 78 ± 14 g DM m^{-2} yr^{-1} (F). The B_c was less than a third of B_f. Models 1 and 2 were significantly parameterized (r^2 = 0.51–0.53, p < 0.001) using the field data (n = 144). Although the parameters of d (R_m at 0°) and f (the temperature coefficient of R_m) were almost the same between the two models, the parameter of R_g (c) was smaller for M1. The R_m and R_{ion} peaked in June–July, whereas R_g peaked earlier in June. Annual R_r was estimated to be 215 g C m^{-2} yr^{-1} and accounted for 41% of R_s. The R_r was partitioned into fine root R_g, fine root R_m, coarse root R_m, and fine root R_{ion} by 32, 46, 13 and 9%, respectively.

The two models were significantly fitted to field data. Although all parameters in M1 were significant determined in both experiments, those from E2 would be more robust because of more data sets for curve fitting and the addition of spatial distribution of coarse root biomass. The parameters of d and f related to R_m were almost the same between M1 and M2 in E2; the Q_{10} of R_m calculated from parameter f was 2.46–2.61. However, the parameter of c for R_g was lower by 20% in M2, suggesting that R_{ion} was assigned to R_g in M1, because R_{ion} was reported to be proportional to R_g from laboratory experiments. Using M2, we estimated that fine roots account for 87% of total R_r annually, and fine root R_r was partitioned into R_g, R_m, and R_{ion} by 37, 53, and 10%, respectively. The R_g, R_m, and R_{ion} varied according to the seasonal variations of P_f, T_s, and T_r, respectively.

To partition R_r into R_g, R_m, and R_{ion}, we applied modified empirical models and parameterized them using seasonal field data of soil CO_2 efflux, B_f, P_f, B_c, T_s, and T_r measured in a young larch-dominated forest regrowing after the removal of surface organic soil. In such a simplified filed condition, we succeeded in significant partitioning of root respiration in a filed condition. Despite ignoring coarse root growth, the results suggest that our approach is capable of partitioning root respiration.

Contents

1. Introduction

1.1 Background

Net ecosystem production (NEP) is the tiny balance of two huge CO_2 fluxes of gross primary production (GPP) and ecosystem respiration (RE). Soil respiration (R_s) accounts for 30–80% of RE on an annual basis in forest ecosystems (Davidson et al. 2006) but typically 70% in temperate forests (Ryan and Law 2005). On a global scale, R_s (98 Pg C yr^{-1}; (Bond-Lamberty and Thomson 2010)) accounts for about 80% of GPP (123 Pg C yr^{-1}; (Beer et al. 2010)). These facts indicate that R_s plays a crucial role in terrestrial carbon cycles.

The R_s is composed of autotrophic respiration (R_a) and heterotrophic respiration (R_h). The R_a is equivalent to respiration from roots (root respiration: R_r) using photosynthate and non-structural carbohydrates as substrate, whereas R_h is the microbial decomposition of soil organic matter (SOM) and carbohydrates (NSC) derived from roots (Moyano et al. 2009). The R_a and R_h respond to temperature and moisture in a different manner (Scott-Denton, Rosenstiel, and Monson 2006; Lavigne, Foster, and Goodine 2004; Boone et al. 1998). Thus, to examine the environmental response of R_s, R_s has been partitioned into R_r and R_h by root-exclusion methods, such as trenching (Epron 2009). In forest ecosystems, the raio of R_r and R_s (R_r / R_s) ranged between 10 and 90% depending on vegetation types and seasons (Hanson et al. 2000) but typically 45–50% (Subke, Inglima, and Francesca Cotrufo 2006).

Roots are classified into non-woody fine roots and woody coarse roots by anatomical traits and physiological functions. Fine roots are physiologically active apexes of root branches and conventionally defined as thinner roots < 2 mm in diameter (*e.g*. Brunner *et al*., 2013; Finér *et al*., 2011). Fine roots absorb and transport water and nutrients, whereas coarse roots, which are ≥ 2 mm in diameter, transport them and anchor and support their aboveground part. The net primary production (NPP) of fine roots is large and consequently accounted for 22% of global terrestrial NPP (McCormack *et al*., 2015). In boreal forests, although fine root biomass accounted for only 16% of root biomass, 73% of all belowground NPP arose from fine root

NPP (Yuan and Chen, 2010); fine root NPP can be an index of belowground NPP (Yuan and Chen, 2013). Because root turnover rates become faster as root diameter becomes thinner (Yuan and Chen, 2010), fine roots supply a large amount of litter to the soil together with labile exudate, which stimulate soil microbial activities and change soil carbon stock. Majority of soil carbon in forest ecosystems certainly results from fine root turnover (Richter *et al*., 1999). The respiration rate normalized by dry matter was much higher from fine roots than from coarse roots (Makita *et al*. 2012; Rewald *et al*., 2014). When the respiration rate was scaled up based on biomass data, stand-level respiration of fine roots accounted for 50–70% of R_s in plantations of acacia and eucalyptus (Chen *et al*., 2009; Marsden *et al*., 2008). Thus, fine roots are the most important component contributing to belowground carbon dynamics in forest ecosystems (Finér *et al*., 2011). However, the function of fine roots in carbon cycles is not well understood yet (McCormack *et al*., 2015), because the production and turnover of fine roots substantially depend on plant functional types and climates (Lambers *et al*., 2008; Yuan and Chen, 2012). In addition, information is still lacking on belowground phenology (Abramoff and Finzi, 2015).

Fine root respiration has been frequently partitioned into growth (R_g) and maintenance (R_m) components (Amthor, 2000; McCree, 1974; Thornley, 1970; Penning de Vries, 1974), plus occasionally into ion uptake (R_i) (Chapin *et al*., 2011; Johnson, 1990; Lambers *et al*., 2008) to examine belowground phenology and predict root respiration using a simple model, in which R_g, R_m and R_i are proportioned to growth (production), biomass and nutrient uptake of fine roots, respectively. Terrestrial biosphere models, such as Biome-BGC, are adopting the partitioning model (Sun *et al*., 2017). Although there is a criticism that the scientific basis is lacking in the quantitative division between R_g and R_m (Cannell and Thornley, 2000; Sweetlove *et al*., 2013), experimental data indicate that the model is a valuable tool in understanding the carbon balance of plants and the ecological controls on plant respiration (Lambers *et al*., 2008; Chapin *et al*., 2011). The model has been parameterized and verified mostly based on laboratory experiment data taken in the controlled environment (*e.g.* Lambers *et al*., 2008; Thongo M'Bou *et al*. 2010). Only two studies from field experiments reported the partitioning of fine root respiration using the model (George *et al*., 2003; Sun *et al*., 2020). George *et al*. (2003) estimated annual values of R_g, R_m and R_i (due to nitrogen uptake) from a short-term chamber experiment and literature

information. Sun *et al*. (2020) conducted a field experiment for more than a year in adjacent two mature forests: an evergreen spruce plantation and a larch-dominated deciduous forest, which are located next to our study site. They quantified annual R_g and R_m and discussed the difference between the two forests. However, the results can have large uncertainty arising from field conditions, such as a high ratio of coarse roots, rich understory species in the deciduous forest and a high spatial variation in litter accumulation, root density and SOM especially in the deciduous forest, because the forests were mature at the age over 35 years and the deciduous forest was damaged by windthrow. These site conditions probably increased the spatial variation of R_h and the contamination from other roots than fine roots, which resulted in uncertainty in R_r separation from R_s and model parameterization. Although it is a challenge to substantially decrease uncertainty in field experiments, the following site conditions can improve data reliability: 1) homogeneity in tree age, 2) young forest with less litter accumulation and coarse roots, 3) no or little understory species, and 4) a small amount of SOM.

1.2 Objectives

We measured seasonal variations in soil CO_2 efflux and fine root dynamics from 2017 to 2018 and 2019 to 2020 in a young larch-dominated forest, respectively, in two experiments. The forest was regenerating on the topsoil-removed bare ground to meet the above conditions. Using carefully measured field data, the objectives of this study are 1) to continuously separate fine root R_r from total R_s, 2) to robustly parameterize the partitioning model, 3) to partition the R_r into R_g, R_m and R_{ion} using a modified model, and 3) to show the phenological variations of fine root respiration along with fine root production and biomass.

2. Material and method

2.1 Study site

The field experiments were conducted twice in 2017–2018 (Experiment 1) and 2019–2020 (Experiment 2) in a regenerating young forest dominated by Japanese larch (*Larix kaempferi*) with sparse Japanese white birth (*Betula platyphylla*) in Tomakomai national forest, southern Hokkaido, Japan (42°44.27′N, 141°31.42′E, 116 m above sea level by Google Earth). The study site was used to be a larch plantation (Photo 2.1) established on volcanogenous regosol with a high-water permeability but was severely destroyed by a windstorm due to a typhoon in 2004 (Photo 2.2) (Sano et al., 2010); all stems of both fallen and standing trees were removed (Phot 2.3), and then organic surface soil (A horizon) was scraped out together with stumps, coarse woody debris, litter accumulation, regenerating understory species and buried seeds in 2006 (Photo 2.4). Because the B horizon is lacking, unweathered pumice stones (C horizon) have been exposed. Wind-blown seeds of larch and birch first germinated on the C horizon in a horizontal flat place in 2007 and have been growing despite poor nutrients (Photo 2.5). The site was located between two forests used for field experiments by Sun *et al*. (2020). The ground surface was sparsely covered with stunted ground vegetation dominated by red raspberry (*Rubus idaeus*). Aboveground biomass (AGB) of trees taller than 2 m was 16.7, 20.9, 27.3 and 32.8 t ha^{-1}, respectively, from 2017 to 2020 (Fig. 2.1), of which larch trees accounted for 81-87% (Photo 2.6). Tree density, tree height and diameter at 1.3 m height in 2018 were 3380 trees ha^{-1}, 4.27 ± 1.21 m and 3.9 ± 2.2 cm (mean ± 1 standard deviation (SD)), respectively. In 2016, bulk density, total carbon (C) concentration, total nitrogen (N) concentration and C/N ratio were 0.446 ± 0.042 g cm- 3, 15.2 ± 13.8 g kg^{-1}, 0.742 ± 0.794 g kg^{-1} and 24.5 ± 5.8 (mean ± 1 standard deviation (SD)), respectively, for top 15-cm-thick fine soil (< 2 mm). The C concentration showed a decreasing tendency with a distance from tree stems according to the amount of leaf litter fall; the C concentration accounted for about 30% of that of a nearby mature larch-dominated forest studied by Sun *et al*. (2020).

Decadal mean annual air temperature and precipitation were 8.1 ± 0.3°C and 1305 ± 202 mm yr^{-1}, respectively, from 2011 to 2020 at a meteorological station (Tomakomai) 14 km

apart from the study site. The highest and lowest monthly mean air temperatures in the same decade were 21.0°C in August and -3.9°C in January, respectively. Snow usually covers the ground for about four months between early December and early April.

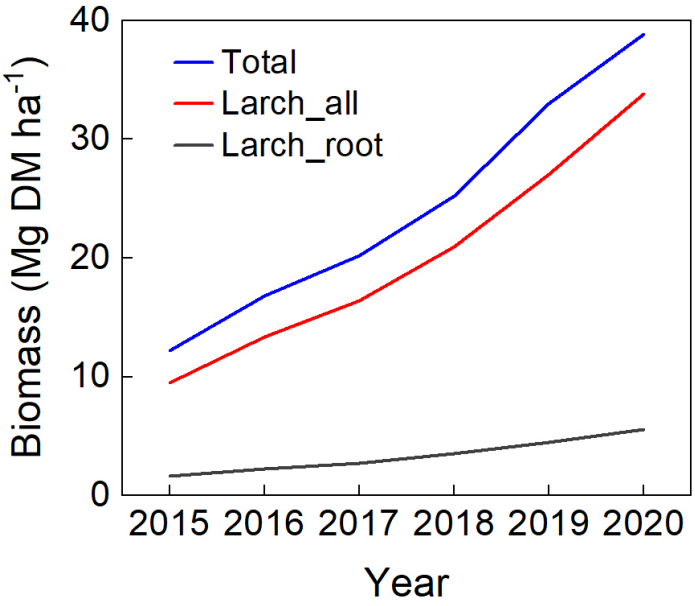

Fig. 2.1 Interannual variation in forest total biomass, larch biomass and larch root biomass from 2015 to 2020.

Photo 2.1 The larch forest before typhoon disturbance

Photo 2.2 The study site just after typhoon disturbance (September 2004)

Photo 2.3 The study site after the removal of fallen trees (May 2005).

Photo 2.4 The study site after the surface soil removal（May 2007).

Photo 2.5 Regrowing visitation (June 2010).

Photo 2.6 Larch-dominated young forest (June 2017).

2.2 Experimental design

2.2.1 Experiment 1 (2017–2018)

Ten pairs of aluminum collars were installed in May 2017 around isolated larch trees. Six pairs of collars were set at 0.5 m (Near), and the others were set at 1.0 m (Far) from the target larch stems (Photo 2.7). The other trees were more than 1.5 m away from collars. In each pair, two collars were set at a 0.4 m space on the bare ground without ground vegetation. Collars were 0.5 m × 0.5 m in size and inserted 3 cm deep into the soil. We trenched a collar (TC) of each pair in early July 2017 by inserting four PVC boards 20 cm deep into the soil around the collar to exclude root respiration. We found by eye from soil profiles that almost all roots appeared in the top 15 cm layer. The other collar (CC) was used for fine root sampling without trenching.

2.2.2 Experiment 2 (2019–2020)

All collars in Experiment 1 were relocated in July 2019. Nine pairs of two collars with a 0.4 m space were installed at 0.5 m (Near) and at 1.0 m (Far) from the target larch stems, respectively. Similarly with Experiment 1, collars were 0.5 m× 0.5 m in size and inserted 3 cm deep into the soil. Of each pair, one collar was trenched (TC) and another was for control (CC).

Photo 2.7 Collars were set at 0.5 m (Near), and the others were set at 1.0 m (Far) from the target larch stems.

Photo 2.8 Collars were set as control (CC) (right) and trench (TC) (left) as a pair.

2.3 Soil CO_2 efflux

Experiment 1 was conducted at intervals of about three weeks between May 2017 and August 2018 with a six-month suspension from mid-November 2017 to mid-May 2018 mainly because of snow. Experiment 2 was conducted with the same interval from August 2019 to November 2020 and suspended during the snow season between mid-November 2019 to mid-April 2020. Soil CO_2 efflux was manually measured on each collar with the same method as in (Sun et al. 2020; Sun, Teramoto, et al. 2017). Young plants germinating in collars were carefully pulled out before measurement, though it was rare. The measurement was conducted between 10:00 and 16:00 on each date with a closed-chamber system equipped with two 0.5-m-tall cubic chambers, an air pump, a datalogger (CR1000; Campbell Scientific Inc., Logan, UT, USA) and a CO_2 analyzer (LI820; Li-Cor Inc., Lincoln, NB, USA) (Photo 2.9). The datalogger was used to control the system and record data. CO_2 concentration in the chamber was measured every 5 s during chamber closing for 3 min. The CO_2 increasing rate was determined from the continuous data by the least squares method, and then soil CO_2 efflux was calculated from the increasing rate and chamber air temperature using the following equation:

$$R = \frac{VP}{RST}\frac{dC}{dt} \quad (1)$$

where V is the chamber volume (m^3), S is the soil surface area inside the chamber (m^2), P is the air pressure (Pa), T is the air temperature inside the chamber (K), dC/dt is the changing rate of CO_2 concentration (μmol mol^{-1} s^{-1}) determined using the least-square method, and the R is the gas constant (8.314 Pa m3 K^{-1} mol^{-1}). Soil temperature (T_s) at a depth of 5 cm and volumetric soil water content (SWC) of the top 5-cm soil were measured immediately after the efflux measurement in each collar by a thermometers (MHP; Omega Engineering, Stanford, CA, USA) (Photo 2.8) and a soil moisture sensor (SM150; Delta-T Device Ltd., Cambridge, UK). Also, T_s at a depth of 6 cm and SWC at a depth of 3 cm were monitored at four points at a nearby station 150 m from the study site (Hirano, Suzuki, and Hirata 2017); we used the data measured at an open place where C horizon was exposed like the study site.

After trenching in early July 2017 and lately July 2019, CO_2 efflux from TC (R_{TC})

corresponded to the sum of original R_h and CO_2 emissions through the decomposition of dead roots (R_{DR}) by trenching (Epron 2009). The method to estimate R_{DR} is described later. Meanwhile, CO_2 efflux from CC (R_{CC}) corresponded to total R_s. Although CC was disturbed by soil sampling, its effect on CO_2 efflux was insignificant because sampling area was negligible (Sun et al. 2020). Thus, the sum of fine and coarse root respirations (R_r) was determined for each pair of collars, as $R_r = R_{CC} - R_{TC} - R_{DR}$. Since the distance from a larch tree was the same, two collars in a pair were expected to have similar root density and litter fall.

We applied the following simple exponential model to analyze the effect of T_s (°C) on soil CO_2 efflux (Rc, μmol m^{-2} s^{-1}) on each collar.

$$Rc = a \cdot exp(b \cdot T_s) \qquad (2)$$

where a and b are fitting parameters. From the temperature response parameter (b), we calculated Q_{10}, which is the factor by which R_c increases with a 10°C temperature rise. In addition, the effect of SWC was analyzed using the temperature-normalized R_c at a base temperature (T_b).

$$R_b = R_c \cdot exp\big(b \cdot (T_b - T_s)\big) \qquad (3)$$

In this study T_b was set at 15°C, mean T_s for the snow-free season. Using the relationship of R_c with T_s and/or SWC, R_{CC} and R_{TC} were calculated half hourly on every collar from the monitoring data of T_s and/or SWC. Daily R_r was calculated for each pair from daily R_{SC}, R_{TC} and R_{DR}.

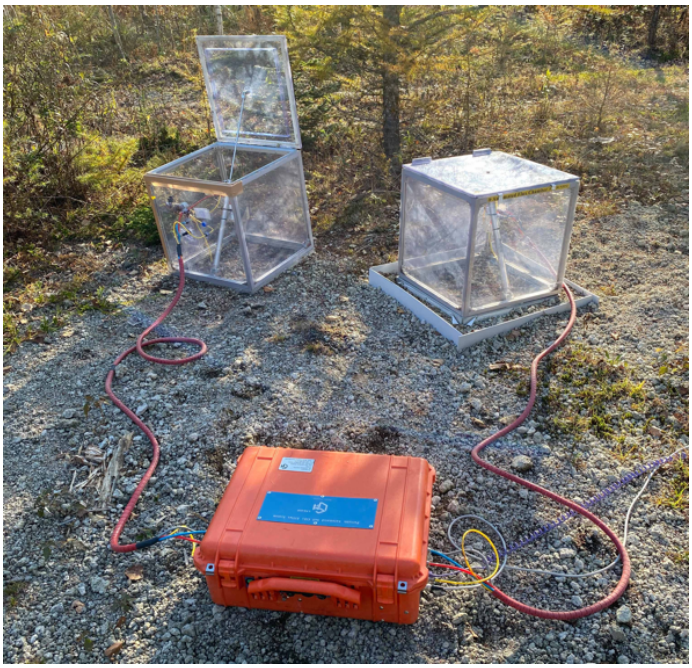

Photo 2.8 The chamber system.

2.4. Decomposition of dead roots

We conducted a root litter bag experiment to determine the decay constant (k) (Gholz *et al*., 2000; Silver and Miya, 2001; Sun *et al*. 2020). In June 2017, we collected topsoil to a depth of 15 cm from the total area of 1 m^2 and extracted fine toots from mixed soil samples with the same method as described later. The root samples were air-dried and weighed, and then some were oven dried. We determined the water content of air-dried samples from the dry weight and calculated the dry weight of air-dried samples. Air-dried samples corresponding to 0.48 g of dry weight were put into each 2-mm mesh bag of 10 cm × 10 cm in size. The sample amount was equivalent to measured root density. A total of 60 bags were buried at a depth of 10 cm at about 1 m from a larch stem in July 2017 (Photo 2.9). Ten bags were collected six times until October 2018, and remaining samples were oven-dried and weighed. The k was determined by fitting the following equation (Wieder and Lang, 1982) to the data.

$$Y = Y_0 \cdot exp(-k \cdot t) \qquad (4)$$

where Y is the dry weight of remaining root samples in bags (g bag^{-1}) at elapsed time t (days), Y_0 the initial dry weight of root samples (0.48 g bag^{-1}) and k the decay constant (d^{-1}). As for the k of coarse roots, we used a reported value of 4.4 × 10^{-4} d^{-1} (= 0.16 yr^{-1}) from a nearby larch-dominated forest (Sun et al. 2020).

The R_{DR} (g C m^{-2} d^{-1}) at elapsed time t (days) was calculated daily, separately for fine and coarse roots using the following equation.

$$R_{DR} = C_c \cdot (X_{t-1} - X_t) = c \cdot X_0 \cdot \exp(-k \cdot t) \cdot \{\exp(k) - 1\} \quad (5)$$

where C_c is the carbon concentration of roots (g g^{-1}), X_t the dry weight of remaining dead roots (g m^{-2}) at t and X_0 the initial dry weight of dead roots (g m^{-2}). For both fine and coarse roots, we used C_c of 0.484 g g^{-1} (Neumann *et al*., 2020), which was the average value of fine roots in European forests. The X_0 of fine roots were set at 66 (Near) and 29 (Far) g m^{-2}, which were based on fine root biomass measured by soil core sampling from CC in July 2017. As for coarse roots, X_0 were determined to be 55 (Near) and 49 (Far) g m^{-2} from soil sampling down to 15 cm in May and September 2019.

Photo 2.9 Litter bags were burned in July 2017.

2.5. Biomass and production of fine roots

The biomass and production of fine roots were measured with the same method as in Sun *et al*. (2020). Fine root biomass density (B_f, g m^{-2}) was measured by soil coring five times from July 2017 to August 2018 for about 14 months with a six-month suspension from mid-November 2017 to mid-May 2018 in Experiment 1. In Experiment 2, the measurement was conducted from September 2019 to November 2020 with the snow season suspension. Soil cores were extracted down to 15 cm with a stainless-steel edged tube with an inner diameter of 2.4 cm (Photo 10). We sampled three cores from each CC every time, using perforated board for positioning. Sampling positions were randomly selected from a grid with 8 cm spacing and not reused. In total, the pit area by sampling amounted to 68 cm^2 for each CC, which accounted for only 2.7% of each collar area. Soil samples were put into PVC tubes and stored in a freezer, and then dispersed in a vat filled with tap water. Only living fine roots with a diameter < 2 mm were visually extracted, dried at 70°C for 48 hours and weighed. The fine roots should have originated from larch trees because the other plants did not exist in the vicinity.

Fine root production rates (P_f, g m^{-2} $period^{-1}$) were measured by the ingrowth core method (*e.g.* Vogt *et al*., 1998) with plastic hair curlers wrapped in a 2 mm mesh sheet. The cores were 20 cm long and had a diameter of 2.3 cm. Air-dried fine soil, which was collected from the study site and sieved through 2 mm meshes, was put into the cores up to 15 cm. For each CC, three cores were inserted down to 15 cm into the pits made by soil core sampling (Photo 11), and three cores inserted previously were collected simultaneously with the core sampling. Collected ingrowth cores were put into PVC tubes and stored in a freezer, and then dry weight of fine roots was determined with the same method as described above. Fine roots penetrate root-free soil in ingrowth cores through meshes during a period between two sampling dates. Thus, the dry weight of fine roots in ingrowth cores corresponds to P_f. Also, annual fine root mortality (M_f, g m^{-2} yr^{-1}) was calculated as a difference between annual P_f and an annual difference in B_f (ΔB_f) ($M_f = P_f - \Delta B_f$). We converted dry weight to carbon using a factor of 0.484. In addition, turnover rates were calculated as the ratio of annual P_f and mean B_f (Brunner *et al*., 2013).

Photo 2.10 Sequential soil core sampling method.

Photo 2.11 Ingrowth core method.

2.6. Sap flow

Sap flow velocity was measured for three trees of a normal size by the thermal dispersion method (Granier, 1987) only in Experiment 2 form July 2019 to November 2020 with a suspension during the leafless season between mid-November 2019 and mid-April 2020 (Table 2.1). Sap flow sensors (CUP-SPF-M, Climatec Inc., Tokyo, Japan) were installed at a height 25 cm below the lowest branch to measure whole transpiration of each tree (Photo 2.12). From a destructive sampling of some trees in the study site, we presumed that the stem area (25–72 cm^2) at the sensor heigh was occupies by sap area. Thus, sap flow rates were calculated as the product of sap flow velocity and the stem area. Although sap flow rates, transpiration rates and water uptake rates by roots are not the same exactly, they are almost the same on a daily basis.

Because diameters at breast height (DBH) were 54.4 ± 28.3 and 58.2 ± 30.4 cm (mean ± 1 SD; n = 215–225) for larch trees in the study site in 2019 and 2020, respectively, the three trees were almost within the range of mean ± 1 SD in DBH. Coarse root biomass was estimated from DBH using an allometric equation for each tree (Table 2.1), and fine root biomass (diameter < 2 mm) was estimated from the coarse root biomass using a ratio between fine and coarse root biomass of 0.185, which was determined for boreal trees (Yuan and Chen, 2010). Daily sap flow rates were normalized by the fine root biomass (T_r, g H_2O g dry matter $(DM)^{-1}$ d^{-1}) to estimate daily water uptake rates by fine roots in each CC.

Table 2.1 Specifics of sample trees, in which sap flow sensors were installed.

Tree	DBH (mm)		Total biomass (kg DM)		Coarse root biomass (kg DM)		Fine root biomass (kg DM)	
	2019	2020	2019	2020	2019	2020	2019	2020
531	36.9	42.5	5.9	7.8	1.02	1.34	0.19	0.25
A514	63.9	71.3	16.2	20.3	2.73	3.38	0.50	0.63
A513	88.9	94.8	25.9	31.9	4.28	5.22	0.79	0.97

Photo 2.12 Sap flow sensor installation

2.7. Partitioning root respiration

Originally, R_r was partitioned into R_g and R_m by the following equation (Amthor 2000; Thornley 1970).

$$R_r = R_g + R_m = g_R \cdot P_f + m_R \cdot B_f \qquad (6)$$

where g_R is the growth respiration coefficient and m_R the maintenance respiration coefficient. We modified the equation as follows, considering field conditions.

$$R_r = R_g + R_m = c \cdot P_f + d \cdot exp(f \cdot T_s) \cdot \left(B_f + B_c\right) : \text{ Model 1} \qquad (7)$$

$$R_r = R_g + R_m + R_{ion} = c \cdot P_f + d \cdot exp(f \cdot T_s) \cdot \left(B_f + B_c\right) + g \cdot T_r \cdot B_f : \text{ Model 2} \quad (8)$$

where c corresponds to g_R (g C g DM^{-1}), d the R_m of unit biomass at 0°C (g C g DM^{-1} d^{-1}), f a temperature coefficient ($°C^{-1}$), B_c coarse root biomass (g m^{-2}), g a transpiration coefficient (g C g H_2O^{-1}), T_r daily sap flow rate per unit fine root biomass (g H_2O g DM^{-1} d^{-1}). In Model 2, respiration for ion uptake (R_{ion}, g C m^{-2} d^{-1}) was introduced. We added temperature effect on R_m in an exponential form, because temperature directly affect R_m (Moyano et al. 2009; Thornley 2011). Although tree survey suggested that coarse roots had grown during the study period, we assumed that the contribution of coarse roots to R_g was negligible because of no available data. However, we incorporated B_c into the second term on the assumption that coarse roots showed the same temperature response as fine roots. We assumed that R_{ion} is proportional to water uptake in the condition of low root density, such as in our study site (Oyewole et al., 2014; Henriksson et al., 2021).

We determined the parameters of c, d, f and g by curve fitting to measured data of R_r, P_f, T_s, B_f, B_c and T_r. For the fitting, mean daily R_r (g C m^{-2} d^{-1}) for each period of core sampling intervals was used. The P_f was converted to daily value (g m^{-2} d^{-1}). The B_f (g m^{-2}) was a mean of two consecutive data measured at the beginning and the end of the period. The T_s (°C) was mean soil temperature for the period. The B_c were set at 55 and 49 g m^{-2} at Near and Far in Experiment 1, and B_c measured in each CC were used in Experiment 2, neglecting its seasonal variation. All the data were prepared from each pair of collars (n = 10 (Experiment 1) and 18 (Experiment 2)) for each period (n = 5 (Experiment 1) and 8 (Experiment 2)). Thus, the data size for curve fitting was 50 and 144 in Experiment 1 and Experiment 2, respectively. In comparison with the previous study (Sun et al. 2020), the data size for curve fitting increased considerably from five to 50 or 144 to obtain a robust result. In addition, we incorporated B_c in the second term, considering the temperature response of R_m of coarse roots and deleted a constant term (h), which represented the respiration of coarse roots and herbaceous roots. In addition, we added R_{ion} in Model 2 for Experiment 2.

2.8. Statistical analysis

We applied Student's *t*-test to compare two means, assuming homoscedasticity. Also, we applied two-way repeated measures ANOVA to test the effects of factors. The significance of curve fitting and parameters were tested using *F*-test and *t*-test, respectively. All the statistical analyses were conducted with a software package (Origin Pro 2015 J; Origin Lab Corporation, Northampton, MA, USA).

3. Results

3.1 Experiment 1 (2017–2018)

3.1.1 Environmental conditions

We conducted a field experiment on fine root dynamics from July 2017 to August 2018. During the annual period between August 2017 and July 2018, mean air temperature and total precipitation were 7.7°C and 1425 mm at the Tomakomai meteorological station. The annual mean air temperature was low beyond the range of its decadal mean ± 1 SD (8.1 ± 0.3°C) between 2010 and 2019, whereas annual precipitation was within the decadal range (1346 ± 159 mm yr^{-1}). The T_s at a depth of 6 cm showed an obvious seasonal variation with the maximum of 27.4°C in mid-July 2017 and the minimum of -0.64°C in early December 2017 on a daily basis (Fig. 1a). Under snow cover, T_s was stable at -0.26 0.14°C between December and February. The SWC at 3 cm increased to 0.21 m^3 m^{-3} in late November and rapidly decreased by soil freezing in December (Fig. 3.1b). In January and February, SWC was stable at 0.067 ± 0.005 m^3 m^{-3}, and then gradually increased in March with the thaw of frozen soil.

Soil temperature measured simultaneously with flux measurement was not significantly different between positions nor between treatments (Table 3.1). Meanwhile, SWC was significantly lower at Far positions ($p < 0.05$).

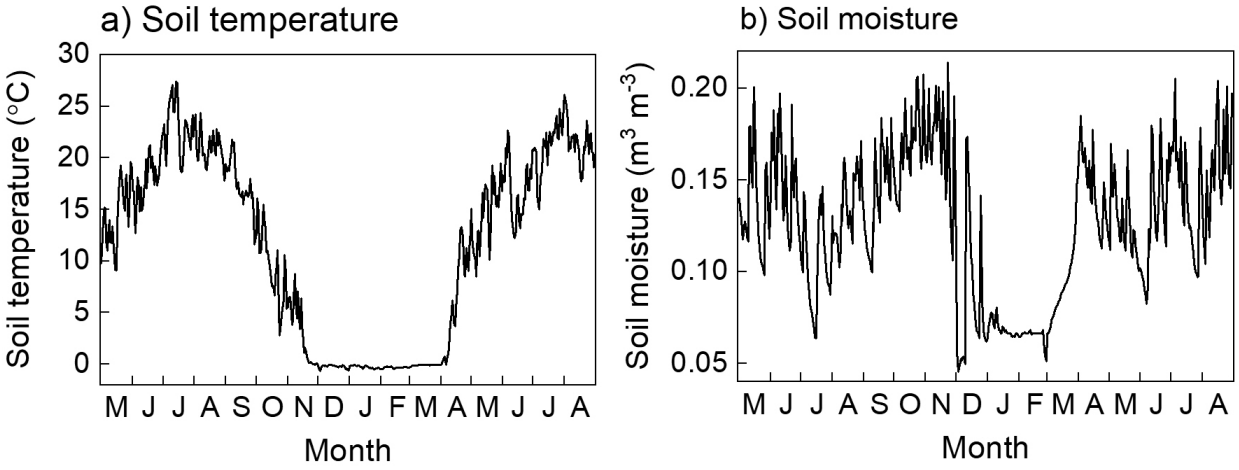

Fig. 3.1. Temporal variations in daily means of soil temperature (T_s) at a depth of 6 cm (a) and volumetric soil water content (SWC) at a depth of 3 cm (b) measured at a nearby station 150 m from the study site from May 2017 to August 2018.

Table 3.1. Soil temperature (T_s) at a depth of 5 cm and volumetric soil water content (SWC) of the top 5-cm soil measured in each collar immediately after CO_2 efflux measurement. Means (± 1 standard deviation) were shown in each cell. Two-way repeated measure ANOVA was applied.

Position	Treatment	T_s (°C)	SWC (m^3 m^{-3})
Near	Control	20.4 ± 7.1	0.097 ± 0.024
	Trenched	19.5 ± 6.9	0.088 ± 0.018
Far	Control	20.7 ± 7.4	0.079 ± 0.022
	Trenched	19.8 ± 7.2	0.080 ± 0.016
ANOVA (*p*-value)	Position	0.89	0.018
	Treatment	0.65	0.44
	Interaction	0.99	0.36

3.1.2. Soil CO_2 efflux

Soil CO_2 efflux (R_c) was measured three and 15 times, respectively, before and after trenching in early July 2017 (Fig. 3.2). Overall, R_c varied according to a seasonal variation in T_s (Fig. 3.1). Before trenching, no significant difference was found between CC and TC in all pairs ($p > 0.05$), which suggested that initial R_c was almost the same in each pair. Meanwhile, significant difference was found between the two collars in all pairs ($p < 0.05$) after trenching. Mean R_c after trenching was 2.41 ± 1.50 (CC) and 1.54 ± 1.11 (TC) μmol m^{-2} s^{-1} at Near and 1.69 ± 0.90 (CC) and 1.30 ± 0.70 (TC) μmol m^{-2} s^{-1} at Far. The R_c showed a significant positive exponential relationship with T_s (Eq. 2) on each collar ($p < 0.05$). Figure 3.3 resulted from mean R_c on each measuring date after trenching. The Q_{10} values were 2.01 (CC) and 2.39 (TC) at Near and 1.58 (CC) and 1.62 (TC) at Far for T_s at a depth of 5 cm. In contrast, no significant linear nor curvilinear relationship was found between temperature-normalized R_c (R_b, Eq. 3) and SWC (data not shown). Thus, we estimate R_{CC} and R_{TC} half hourly for every pair of collars from T_s monitoring data using Eq. 2.

The result of the root litter bag experiment is shown in Fig. 3.4. A negative exponential equation (Eq. 4) was fitted to the data in 2017 and 2018 separately, because no change was measured in the winter between mid-November and mid-May. The k values before mid-November and after mid-May were 2.1 × 10^{-3} (r^2 = 0.88) and 1.7 × 10^{-3} d^{-1} (r^2 = 0.97), respectively. We set k at 0 in the winter. If the equation is fitted to all data, k is calculated to be 1.00 × 10^{-3} d^{-1} (r^2 = 0.71), which is equivalent to 0.36 yr^{-1}.

Daily R_{DR} was calculated from the k values using Eq. 5, and then daily R_s (R_{CC}) was partitioned into R_h and R_r of all roots (Fig. 3.5). Since R_{CC} and R_{TC} were estimated from T_s, all respiration components varied according to the seasonal variation of T_s (Fig. 3.1). Under snow, R_s, R_h and R_r were stable at 0.61, 0.37 and 0.24 g C m^{-2} d^{-1}, respectively, at Near and 0.42, 0.33 and 0.08 g C m^{-2} d^{-1}, respectively, at Far, which indicates that the ratios of R_r to R_s were 0.39 and 0.19, respectively, at Near and Far under snow. The R_m of coarse roots (R_{m_coarse}) was calculated using Eq. 6. Thus, the difference between R_r and R_{m_coarse} correspond to R_r of fine

roots, which were 0.20 and 0.04 g C m^{-2} d^{-1}, respectively, at Near and Far under snow. Annual CO_2 efflux was calculated between August 2017 and July 2018 (Table 3.2). All the CO_2 effluxes were larger at Near than at Far, though only R_{CC} was significantly different ($p < 0.05$). The ratios (Far / Near) of R_{CC} (R_s), R_h and R_r were 0.63, 0.83 and 0.28, respectively. The R_{DR} accounted for 3% of R_s at both positions. The R_r accounted for 37 and 16% of R_s, respectively, at Near and Far.

Similarly, measured R_{CC} was partitioned into R_h and R_r for each collar pair. The R_h and R_r significantly responded to T_s ($p < 0.05$) according to Eq. 2. The Q_{10} values of R_h and R_r were 2.02 ± 1.28 and 2.01 ± 1.21 (mean ± 1 SD), respectively, at Near ($n = 6$) and 2.15 ± 1.20 and 2.14 ± 1.29, respectively, at Far ($n = 4$). No significant difference was found between R_h and R_r at both positions.

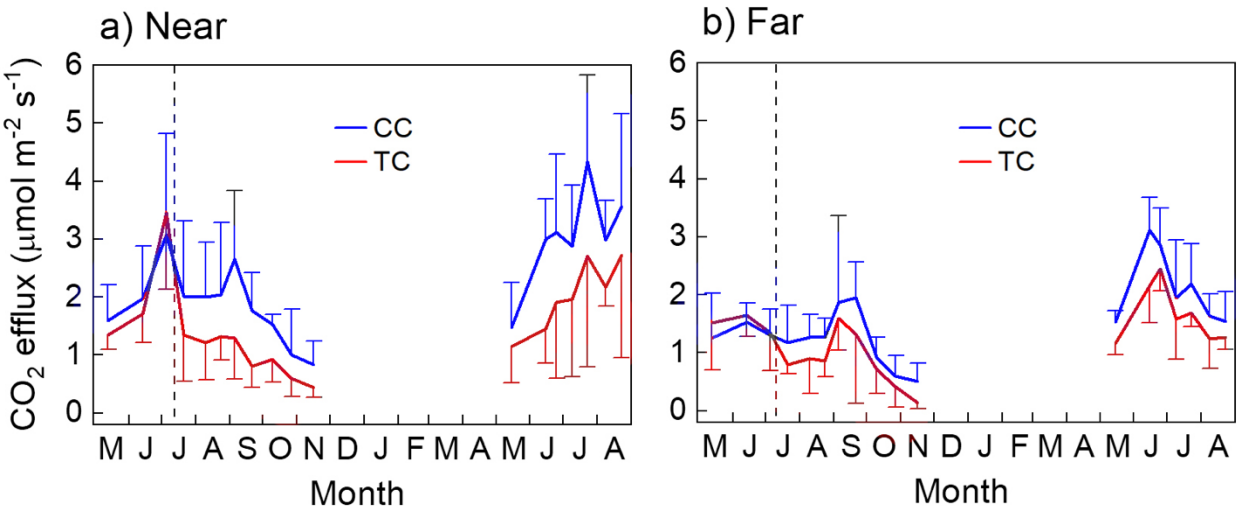

Fig. 3.2. Temporal variations in soil CO_2 efflux (R_c) in control collars (CC) and trenched collars (TC) at Near ($n = 6$) (a) and Far ($n = 4$) (b) from May 2017 to August 2018. Vertical bars denote 1 standard deviation. The dashed vertical lines denote the time of trenching.

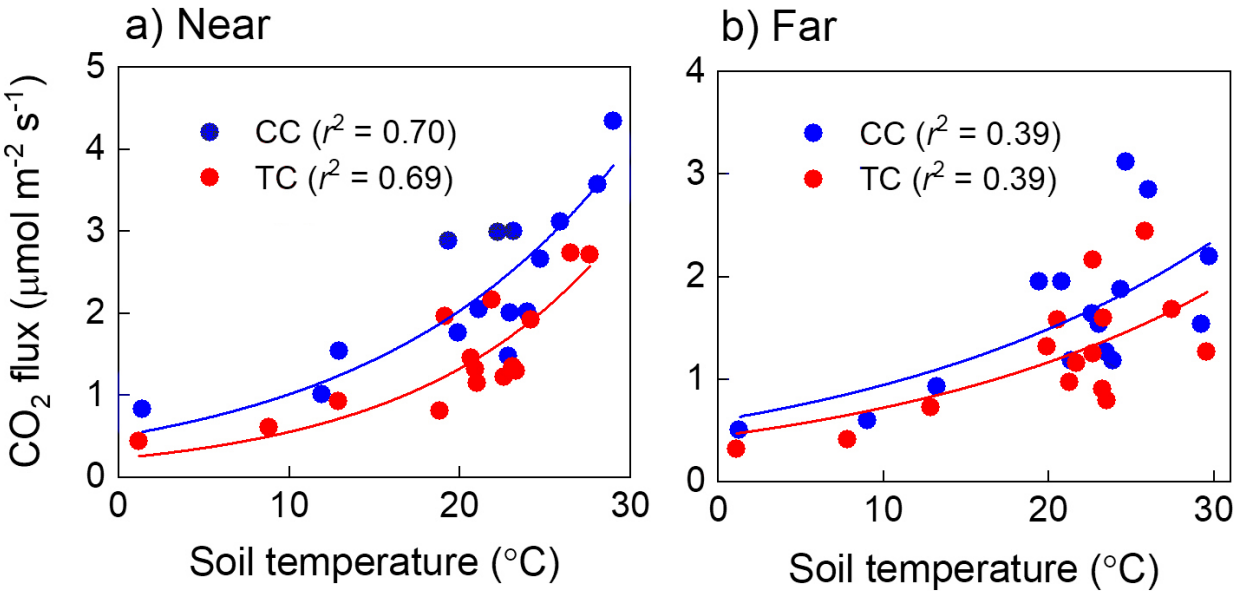

Fig. 3.3. Relationship of soil CO_2 efflux (R_s) with soil temperature (T_s) in collars for root sampling (CC) and trenched collars (TC) at Near (n = 6) (a) and Far (n = 4) (b) from May 2017 to August 2018. An exponential curve (Eq. 1) was significantly fitted; r^2 values were shown.

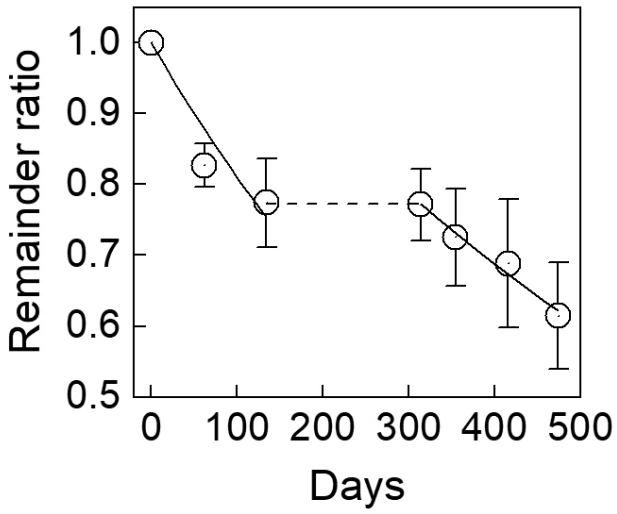

Fig. 3.4. Temporal variation in fine root litter left in root litter bags (remainder ratio) from July 2017 to October 2018. Means (± 1 standard deviation) were plotted (n = 10). A negative exponential equation (Eq. 4) was separately fitted to data in 2017 and 2018. No change was found in fine root litter between mid-November 2017 and mid-May 2018 (dashed line).

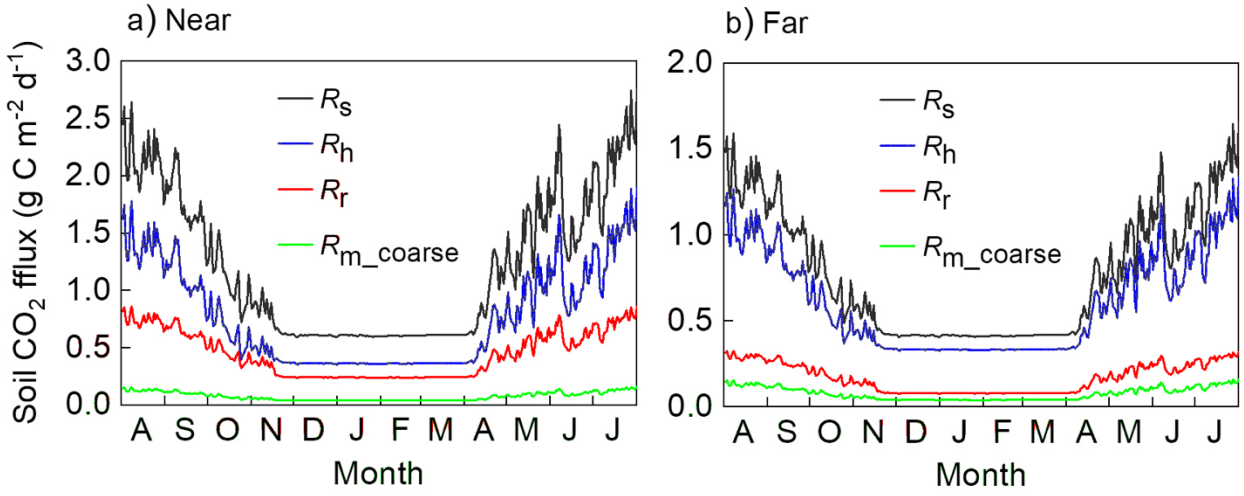

Fig. 3.5. Temporal variations in mean daily soil respiration (R_s), heterotrophic respiration (R_h), root respiration (R_r) and coarse root maintenance respiration (R_{m_coarse}) at Near (n = 6) (a) and Far (n = 4) (b) calculated from the monitoring data of soil temperature (T_s) between August 2017 and July 2018.

Table 3.2. Annual soil respiration (R_{CC} or R_s), soil CO_2 efflux in trenched collars (R_{TC}), CO_2 emissions through dead root decomposition in trenched collars (R_{DR}), heterotrophic respiration (R_h) and root respiration (R_r) (g C m^{-2} yr^{-1}) at Near (n = 6) and Far (n = 4). Means (± 1 standard deviation) were shown. Numbers in parentheses denote percentages against R_{CC}.

Position	R_{CC}(R_s)	R_{TC}	R_{DR}	R_h	R_r
Near	493 ± 111 (100)	326 ± 75 (66)	13 (3)	313 ± 75 (63)	181 ± 123 (37)
Far	311 ± 68 (100)	269 ± 79 (86)	8 (3)	261 ± 79 (84)	51 ± 34 (16)

3.1.3. Biomass and production of fine roots

Fine root biomass (B_f) at Near showed a small peak in early September 2017, and then tended to increase from November until late August 2018 (Fig. 3.6a). Similarly, B_f at Far showed an increasing tendency in the warm season. In contrast, fine root production (P_f) showed a clear seasonal variation both at Near and Far (Fig. 3.6b); it decreased during the fall and increased during the late spring and summer. In the cold season between mid-November and mid-May, including the snowy season for about four months, P_f was small at 0.035 ± 0.018 and 0.043 ± 0.041 g m^{-2} d^{-1}, respectively, at Near and Far. The P_f showed a significant exponential relationship ($p < 0.05$) with T_s at a depth of 5 cm in the same form as Eq. 2 (Fig. 3.7a), which resulted in Q_{10} values of 4.48 and 2.51, respectively, at Near and Far. The high Q_{10} of 4.48 reflects a large seasonal variation in P_f at Near (Fig. 3.6b). Also, B_f showed a significant exponential relationship ($p < 0.05$), though Q_{10} values were lower with 1.08 and 1.49, respectively, at Near and Far. A significant linear relationship with a slope of 1.20 (r^2 = 0.43, $p < 0.001$) was found between R_r and P_f, regardless of positions (Fig. 3.8a). The relationship between R_r and B_f was also significant ($r^2 = 0.33$, $p < 0.01$) (Fig. 3.8b), whereas P_f was not significantly correlated with B_f ($p > 0.10$). Annually, P_f ($p < 0.05$) and mean B_f ($p <$ 0.01) were significantly larger at Near than Far, whereas the turnover rate ($p < 0.01$) was significantly lower at Near (Table 3.3).

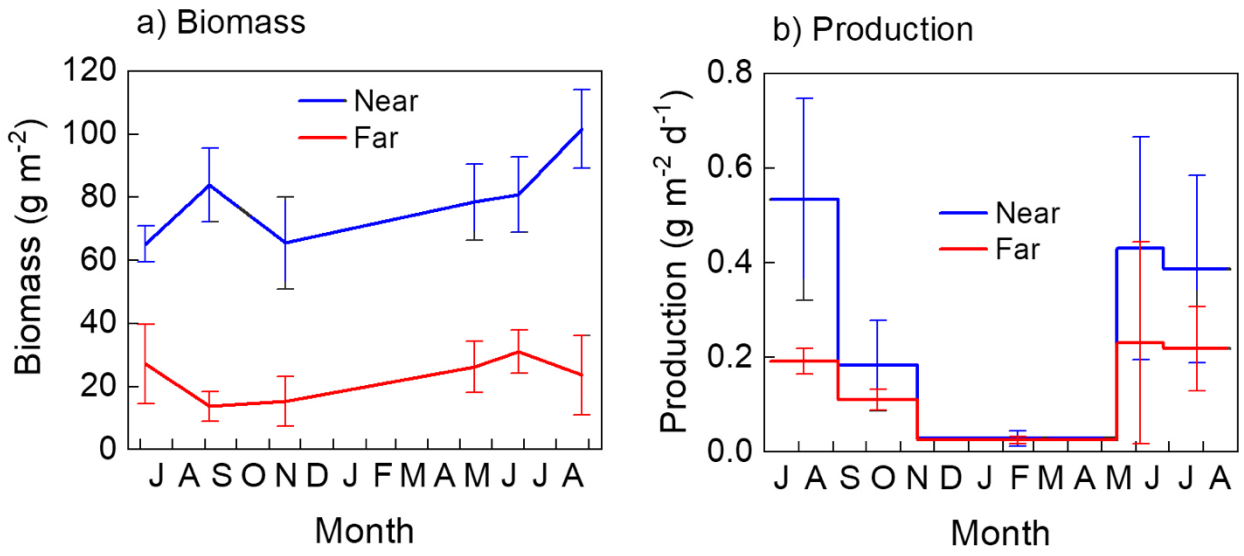

Fig. 3.6. Temporal variations in fine root biomass (B_f) (a) and fine root production (P_f) (b) at Near (n = 6) and Far (n = 4) from July 2017 to August 2018. Means (± 1 standard deviation) were shown.

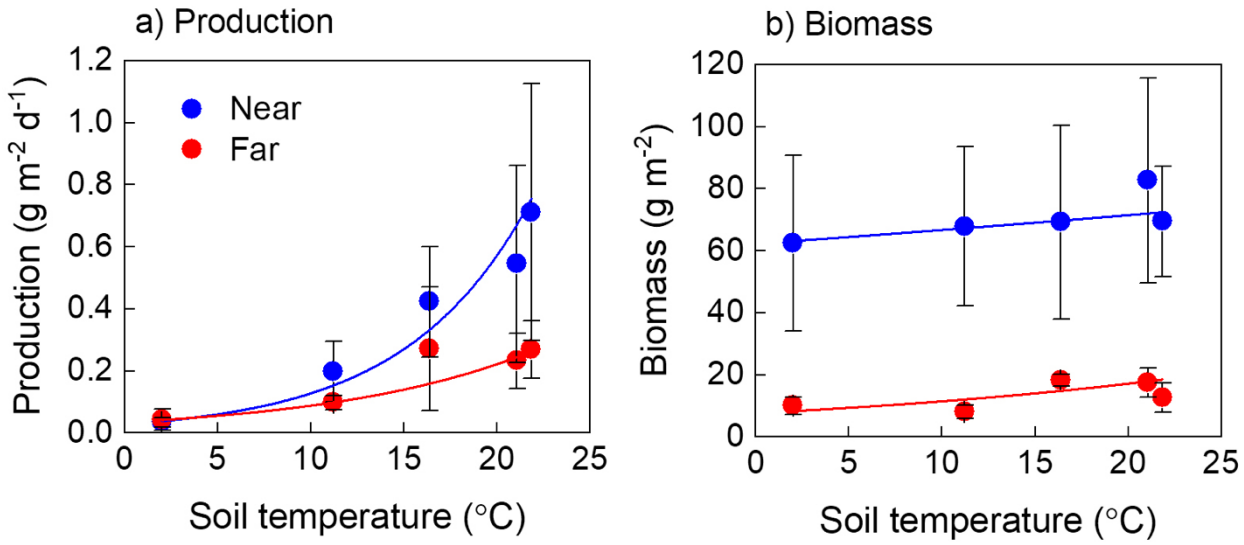

Fig. 3.7. Relationships of fine root production (P_f) with soil temperature (T_s) (a) and fine root biomass (B_f) with soil temperature (T_s) (b) at Near (n = 6) and Far (n = 4). Soil temperature was averaged for each interval of root sampling. Means (± 1 standard deviation) were plotted. An exponential curve (Eq. 1) was significantly fitted.

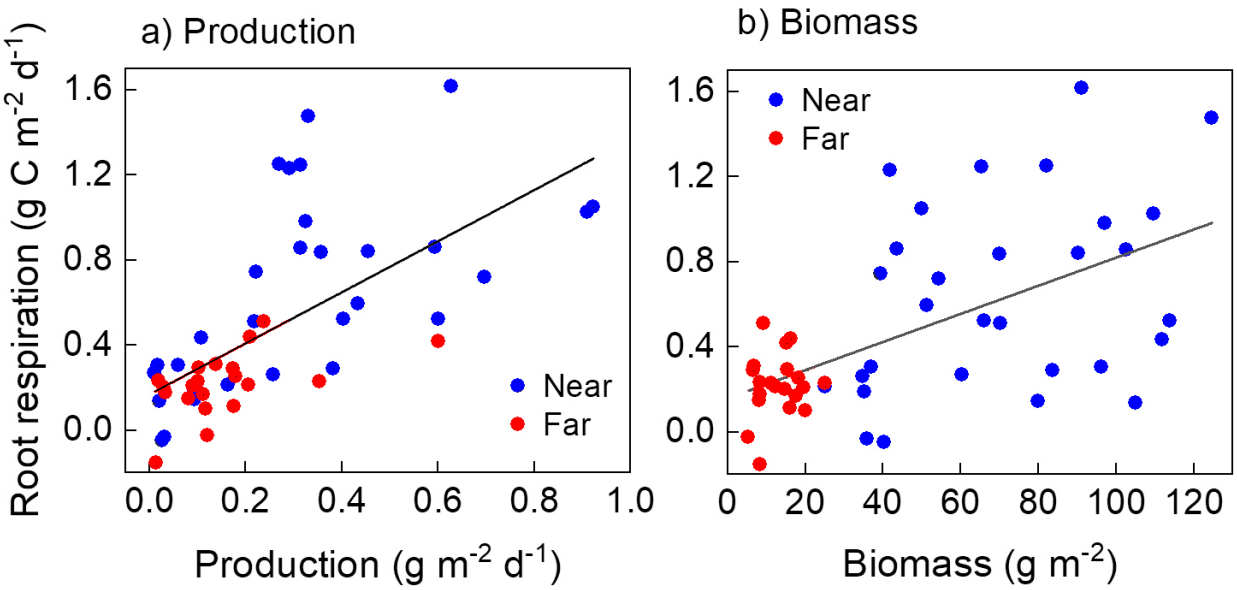

Fig. 3.8. Relationship of root respiration (R_r) with fine root production (P_f) (a) or fine root biomass (B_f) (b) at Near and Far. Root respiration was averaged for each interval of root sampling. A significant regression line was drawn for each scatter plot.

Table 3.3. Annual values of fine root production (P_f), annual increase in fine root biomass (ΔB_f), fine root mortality (M_f), mean fine root biomass (B_f) and fine root turnover rates at Near (n = 6) and Far (n = 4). Means (± 1 standard deviation) were shown.

Posotion	P_f (g m^{-2} y^{-1})	ΔB_f (g m^{-2} y^{-1})	M_f (g m^{-2} y^{-1})	Mean B_f (g m^{-2})	Turnover rate (y^{-1})
Near	81 ± 22	12 ± 33	93 ± 47	70 ± 21	1.27 ± 0.57
Far	41 ± 10	4 ± 5	46 ± 10	13 ± 5	3.26 ± 1.45

3.1.4. Partitioning root respiration

Model 1 (Eq. 6) was significantly fitted to the data set ($p < 0.001$) with an adjusted r^2 of 0.59, respectively (Table 3.4). Using the parameters, we partitioned R_r.

The Q_{10} calculated from the parameter f was 1.7. Annual R_r was partitioned into R_g and R_m using the fitting parameters (Table 3.5). At Near, R_g of fine roots, R_m of fine roots and R_m of coarse roots accounted for 26, 57 and 17% of their sum (estimated R_r), respectively. The bias between R_r from Table 3.2 and the estimated R_r was zero. Meanwhile, R_g, fine root R_m and coarse root R_m accounted for 34, 27 and 39% of their sum at Far; the bias was 19 g C m^{-2} yr^{-1} (37%). The larger bias at Far was partly due to a smaller number of replications at Far ($n = 4$) than at Near ($n = 6$). The R_g and fine root R_m were significantly larger at Near ($p < 0.05$). In addition, the respirations were spatially averaged with a weight of circumference: 3.14 and 6.28 m for Near and Far, respectively. As a result, R_g, fine root R_m and coarse root R_m accounted for 30, 44 and 26% of the total R_r on average in a circumferential area between 0.5 and 1.0 m in radius.

The R_g varied seasonally in parallel with P_f (Figs. 6b and 9), whereas R_m varied mainly according to a seasonal variation in T_s (Figs. 3.1 and 3.9). The contribution of R_g to fine root R_r (= R_g / (R_g + fine root R_m)) was larger at Far with 0.39 in the cold season and 0.59 on average in the warm season than at Near with 0.10 and 0.35, respectively (Fig. 3.9c).

Table 3.4. Fitting parameters of Eq. 6 ($n = 50$) (± 1 standard error) with significance (p value).

	Parameter	p-value
c (g C g DM^{-1})	0.57 ± 0.22	0.012
d (g C g DM^{-1} d^{-1})	0.0021 ± 0.00087	0.022
f ($°C^{-1}$)	0.054 ± 0.021	0.016
Adjusted r^2	0.59	
p-value	< 0.001	

Table 3.5. Annual sums (g C m^{-2} yr^{-1}) of root respiration (R_r) from Table 3.2, fine root growth respiration (R_g), fine root maintenance respiration (R_{m_fine}), coarse root maintenance respiration (R_{m_coarse}) and the sum of R_g, R_{m_fine} and R_{m_coarse} (Sum) at Near (n = 6) and Far (n = 4), which corresponds to R_r. Values at Near and Far were spatially averaged with a weight of circumference: 3.14 and 6.28 m for Near and Far, respectively (weighted average). Means (±1 standard deviation) were shown. Numbers in parentheses denote percentages against Sum.

Position	R_r	R_g	R_{m_fine}	R_{m_coarse}	Sum
Near	181 ± 123	47 ± 12 (26)	104 ± 31 (57)	30 (17)	181 ± 32 (100)
Far	51 ± 34	24 ± 3 (34)	19 ± 4 (27)	27 (39)	70 ± 4 (100)
Weighted average	94	32 (30)	47 (44)	28 (26)	107 (100)

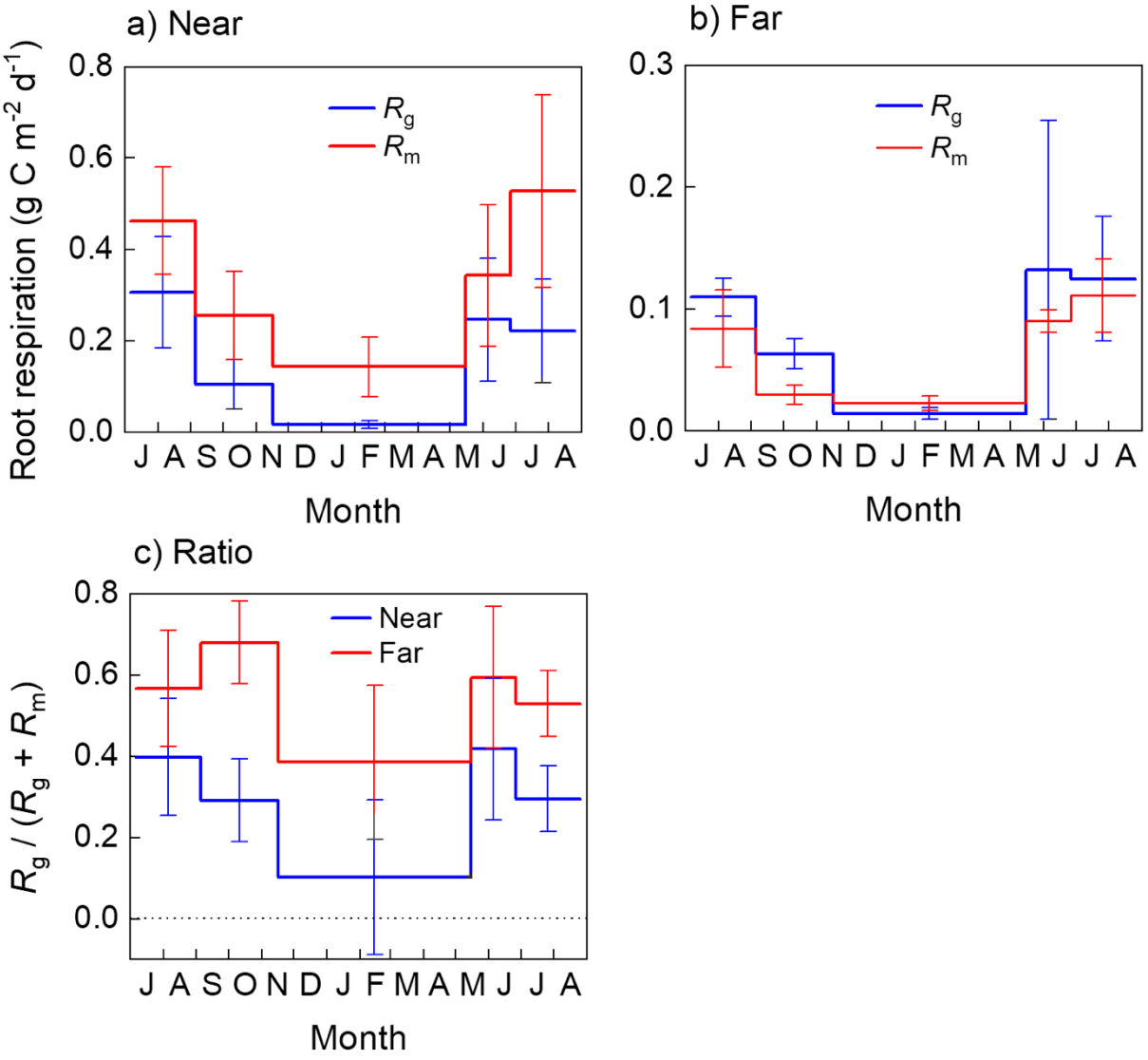

Fig. 3.9. Temporal variations in fine root growth respiration (R_g) and maintenance respiration (R_{m_fine}) at Near (a, n = 6) and Far (b, n = 4), and the ratio of R_g to the sum of R_g and R_m (c) from July 2017 to August 2018. Means (± 1 standard deviation) were shown.

3.2 Experiment 2 (2019–2020)

3.2.1 Environmental conditions

During the annual period between November 2019 and October 2020, mean air temperature and total precipitation were 8.7°C and 968 mm at the Tomakomai meteorological station. The annual mean air temperature was high beyond the range of its decadal mean ± 1 SD (8.1 ± 0.3°C) between 2011 and 2020, whereas annual precipitation was low beyond the decadal range (1305 ± 202 mm yr^{-1}). The T_s at a depth of 6 cm showed an obvious seasonal variation with the maximum of 24.8°C in mid-August 2020 and the minimum of -5.0°C in early January 2020 on a daily basis (Fig. 3.10a). The lower minimum T_s was caused by thin snow accumulation until January. The SWC at 3 cm rapidly decreased by soil freezing in December (Fig. 3.10b). In January and February, SWC was stable at 0.045 ± 0.003 m^3 m^{-3}, and then gradually increased in March. At the end of March, SWC rapidly increased with the thaw of frozen soil.

Soil temperature measured simultaneously with flux measurement was not significantly different between positions nor between treatments (Table 3.1). Meanwhile, SWC was significantly lower in trenched collars (TC) ($p < 0.05$).

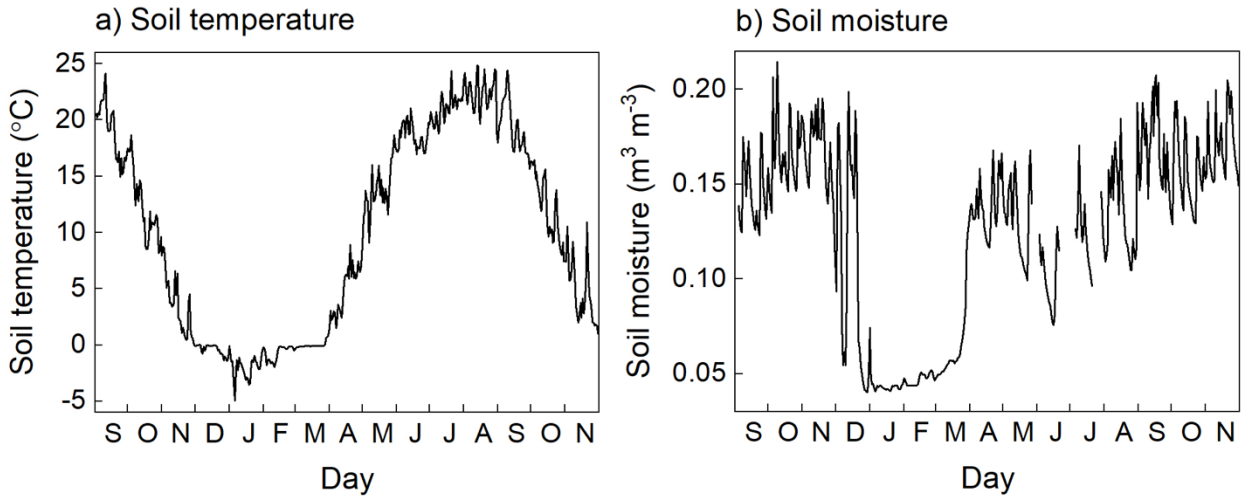

Fig. 3.10. Temporal variations in daily means of soil temperature (T_s) at a depth of 6 cm (a) and volumetric soil water content (SWC) at a depth of 3 cm (b) measured at a nearby station 150 m from the study site from September 2019 and November 2020.

Table 3.6. Soil temperature (T_s) at a depth of 5 cm and volumetric soil water content (SWC) of the top 5-cm soil measured in each collar immediately after CO_2 efflux measurement (n = 9). Means (± 1 standard deviation) were shown in each cell. Two-way repeated measure ANOVA was applied.

Position	Treatment	T_s (°C)	SWC (m^3 m^{-3})
Near	Control	15.4 ± 6.3	0.119 ± 0.051
	Trenched	15.1 ± 6.2	0.110 ± 0.045
Far	Control	15.3 ± 6.7	0.119 ± 0.042
	Trenched	15.1 ± 6.4	0.112 ± 0.038
ANOVA (p-value)	Position	0.96	0.73
	Treatment	0.59	0.035
	Interaction	0.97	0.71

3.2.2. Soil CO_2 efflux

Soil CO_2 efflux (R_c) was measured 16 times. Overall, R_c varied according to a seasonal variation in T_s (Fig. 3.11). Significant difference was found between the two collars in all pairs ($p < 0.05$). In all collars, R_c was significantly related to T_s according to Eq. 2 ($p < 0.05$). The base R_c at 0°C (R_0) was significantly different both between positions and between treatments ($p < 0.05$) (Table 3.7). The R_0 was larger at Near and in CC. Meanwhile, Q_{10} was not significantly different between positions nor between treatments. In contrast, no significant linear nor curvilinear relationship was found between temperature-normalized R_c (R_b, Eq. 3) and SWC (Fig.3.12). Thus, we estimate R_{CC} and R_{TC} half hourly for every pair of collars from T_s monitoring data using Eq. 2.

Daily R_{DR} was calculated from the k values of 1.00×10^{-3} d^{-1} for fine roots (Fig. 3.13) using Eq. 5, and then daily R_s (R_{CC}) was partitioned into R_h and R_r of all roots (Fig. 3.14). Although k values are different between fine and coarse roots (Sun *et al*., 2020), we used the k both for fine and coarse roots.

Since R_{CC} and R_{TC} were estimated from T_s, all respiration components varied according to the seasonal variation of T_s (Fig. 3.10). Under snow, R_s, R_h and R_r were stable at 0.72, 0.39 and

0.33 g C m^{-2} d^{-1}, respectively, at Near and 0.61, 0.28 and 0.33 g C m^{-2} d^{-1}, respectively, at Far, which indicates that the ratios of R_r to R_s were 0.46 and 0.55, respectively, at Near and Far under snow. The R_m of coarse roots (R_{m_coarse}) was calculated using Eq. 6. Thus, the difference between R_r and R_{m_coarse} correspond to R_r of fine roots, which were 0.68 and 0.59 g C m^{-2} d^{-1}, respectively, at Near and Far under snow. Annual CO_2 efflux was calculated between November 2019 and October 2020 (Table 3.8). The ratios (Far / Near) of R_{CC} (R_s), R_h and R_r were 0.78, 0.81 and 0.74, respectively. The total R_{DR} accounted for 4–5% of R_s. The R_r accounted for 45–47% of R_s.

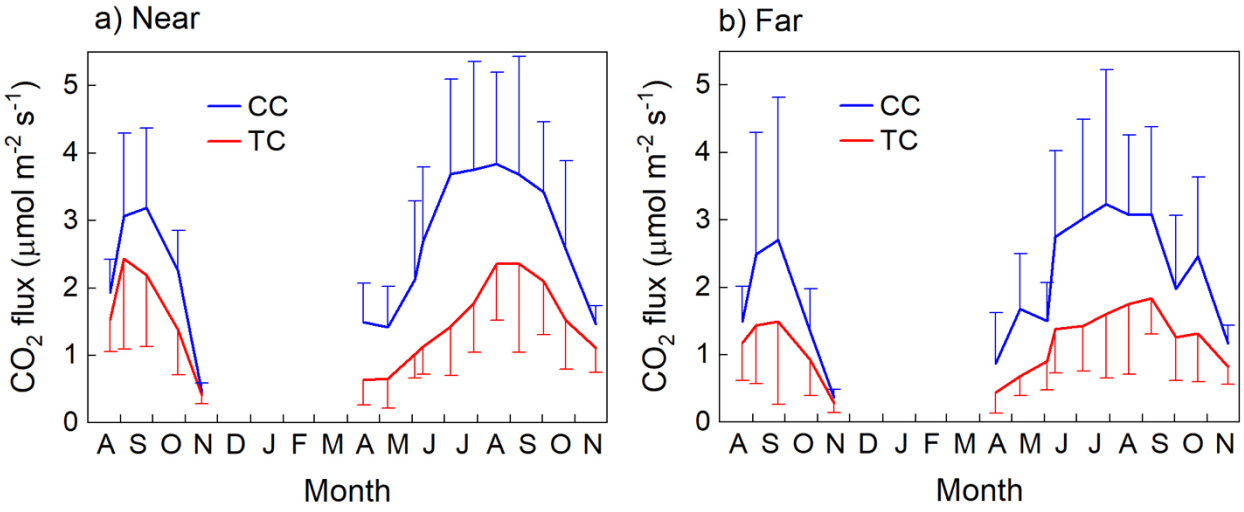

Fig. 3.11. Temporal variations in soil CO_2 efflux (R_c) in control collars (CC) and trenched collars (TC) at Near and Far (n = 9) from August 2019 to November 2020. Vertical bars denote 1 standard deviation.

Table 3.7. Base soil respiration at 0°C (R_0) and Q_{10} determined by Eq. 2. Means ± 1 standard deviation (n = 9) were shown. Two-way repeated measure ANOVA was applied.

Position	Treatment	R_0 (μmol m^{-2} s^{-1})	Q_{10}
Near	Control	0.73 ± 0.18	1.97 ± 0.43
	Trenched	0.49 ± 0.15	1.78 ± 0.28
Far	Control	0.49 ± 0.17	2.13 ± 0.41
	Trenched	0.34 ± 0.16	2.04 ± 0.52
ANOVA (p-value)	Position	0.001	0.139
	Treatment	0.001	0.317
	Interaction	0.404	0.763

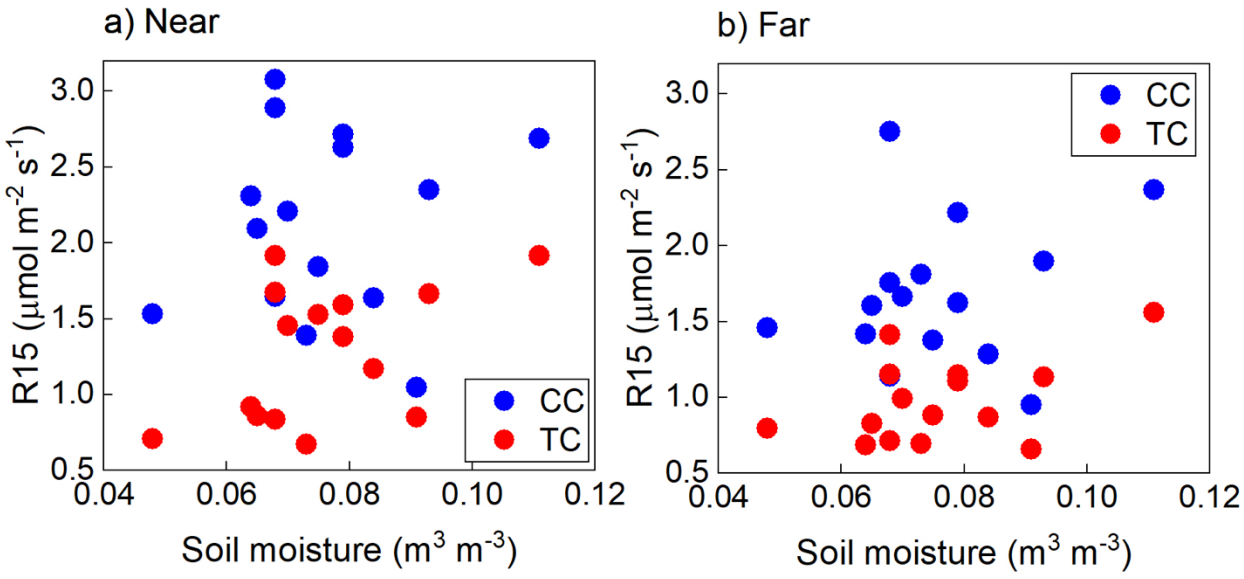

Fig. 3.12. Temperature-normalized R_c (at 15°C) vs. soil moisture (SWC at 3 cm depth).

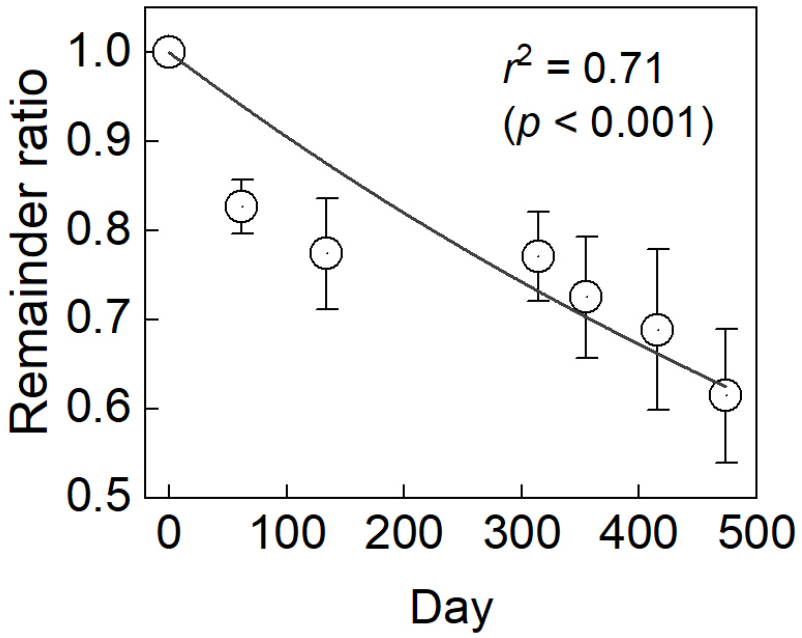

Fig. 3.13. Temporal variation in fine root litter left in root litter bags (remainder ratio) from July 2017 to October 2018. Means ± 1 standard deviation were plotted (n = 10). A negative exponential equation (Eq. 4) was fitted to data in 2017 and 2018. The data are the same as in Fig. 3.4.

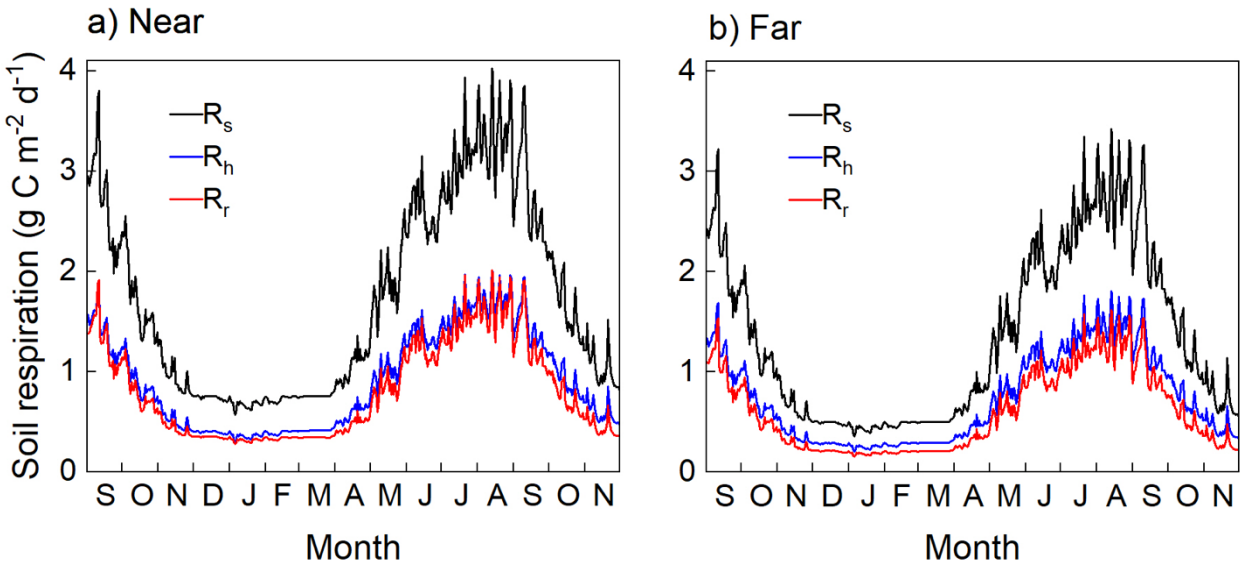

Fig. 3.14. Temporal variations in mean daily soil respiration (R_s), heterotrophic respiration (R_h), root respiration (R_r) at Near and Far (n = 9) calculated from the monitoring data of soil temperature (T_s) between September 2019 and November 2020.

Table 3.8. Annual soil respiration (R_{CC} or R_s), soil CO_2 efflux in trenched collars (R_{TC}), CO_2 emissions through dead root decomposition in trenched collars (R_{DR_fine}, R_{DR_coarse} and R_{DR_all}), heterotrophic respiration (R_h) and root respiration (R_r) (g C m^{-2} yr^{-1}) at Near and Far (n = 9) between November 2019 and October 2020. Means ± 1 standard deviation were shown. Numbers in parentheses denote percentages against R_{CC}.

Position	R_{CC}(R_s)	R_{TC}	R_{DR_fine}	R_{DR_coarse}	R_{DR_all}	R_h	R_r
Near	610 ± 78 (100)	356 ± 73 (58)	27 ± 14 (4.4)	6 ± 6 (1.0)	33 ± 14 (5.4)	323 ± 74 (53)	287 ± 86 (47)
Far	474 ± 155 (100)	282 ± 84 (59)	17 ± 18 (3.5)	3 ± 4 (0.6)	20 ± 20 (4.1)	262 ± 71 (55)	212 ± 104 (45)

3.2.3. Biomass and production of fine roots

Fine root biomass (B_f) at Near showed a small peak in October 2019 and May–July 2020 (Fig. 3.15). Similarly, B_f at Far showed a small peak in September–October 2019 and July 2020, though seasonal variation was not so clear. In contrast, fine root production (P_f) showed a clear seasonal variation both at Near and Far (Fig. 3.16); it sharply decreased in November 2019 and increased in April 2020. In 2020, P_f peaked in early summer and decreased during fall. In the cold season between mid-November and mid-April, P_f was small at 0.11 ± 0.02 and 0.13 ± 0.21 g m^{-2} d^{-1}, respectively, at Near and Far.

Neither B_f nor P_f showed no significant correlation ($p > 0.05$) with T_s (Fig. 3.17). The R_r showed a significant linear relationship both with B_f ($r^2 = 0.16$, $p < 0.001$) and P_f ($r^2 = 0.24$, $p < 0.001$), regardless of positions (Fig. 3.18). The relationship between P_f and B_f was also significant ($r^2 = 0.12$, $p < 0.01$) (data not shown). Annually, only the turnover rate calculated as the ratio of P_r and Mena B_f showed significant difference between positions, which was significantly larger at Far ($p < 0.05$) (Table 3.9).

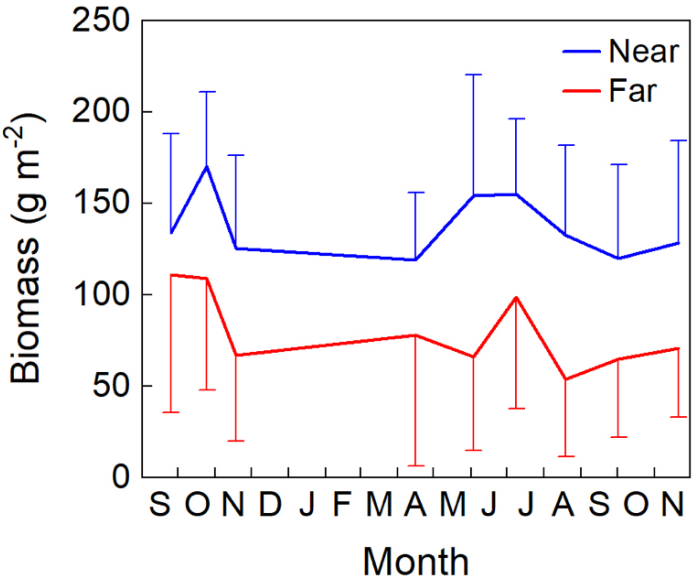

Fig. 3.15. Temporal variations in fine root biomass (B_f) at Near and Far (n = 9) from September 2019 to November 2020. Means ± 1 standard deviation were shown.

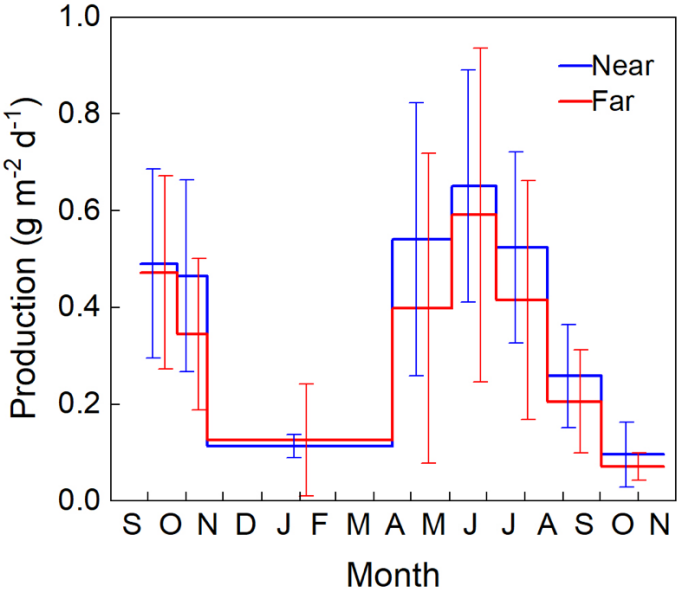

Fig. 3.16. Temporal variations in fine root production (P_f) at Near and Far (n = 9) from September 2019 to November 2020. Means ± 1 standard deviation were shown.

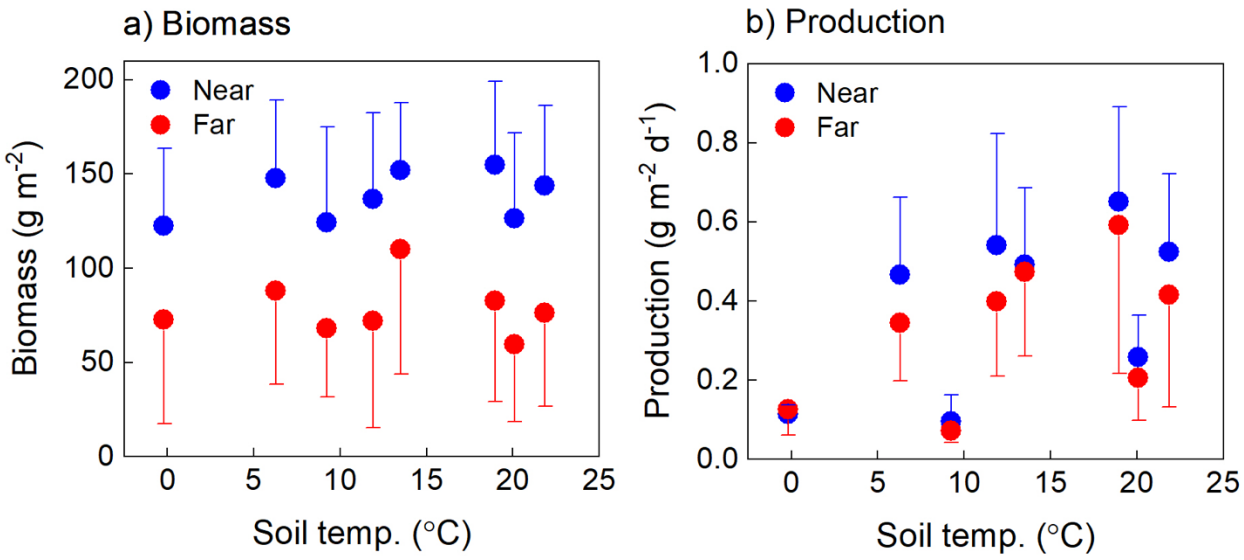

Fig. 3.17. Relationships of fine root biomass (B_f) with soil temperature (T_s) (a) and fine root production (P_f) with soil temperature (T_s) (b) at Near and Far (n = 9). Soil temperature was averaged for each interval of root sampling. Means ± 1 standard deviation were plotted.

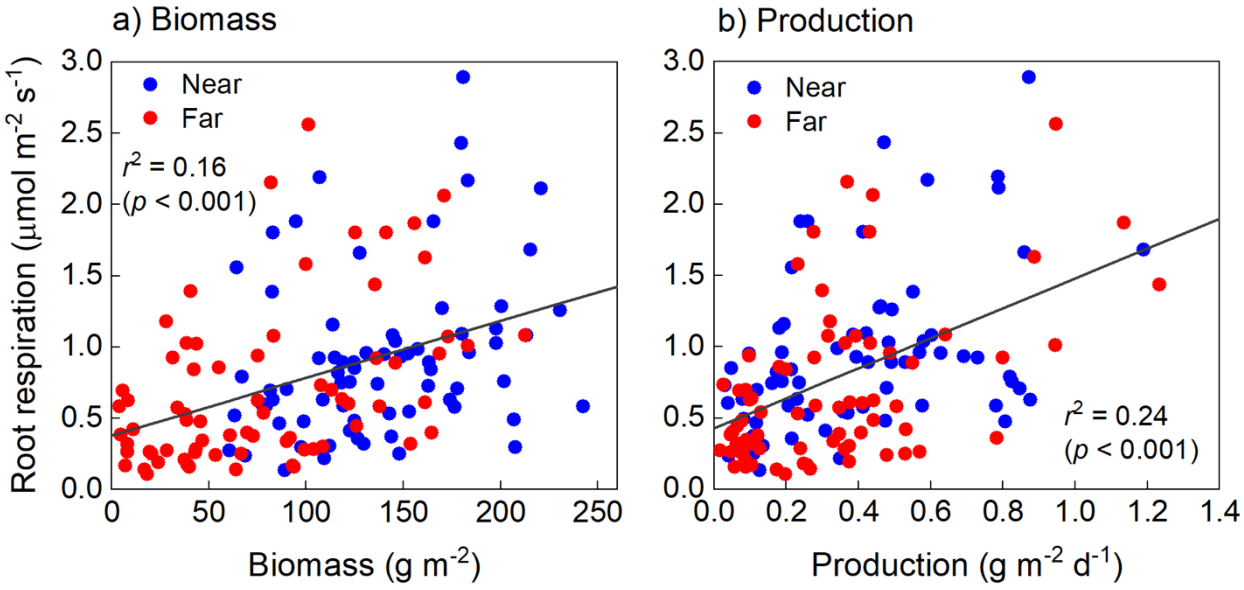

Fig. 3.18. Relationship of root respiration (R_r) with fine root biomass (B_f) (a) or fine root production (P_f) (b) at Near and Far. Root respiration was averaged for each interval of root sampling. A significant regression line was drawn.

Table 3.9. Annual values of fine root production (P_f), annual increase in fine root biomass (ΔB_f), fine root mortality (M_f), mean fine root biomass (B_f), mean coarse root biomass (B_c) and fine root turnover rates at Near and Far (n = 9) between November 2019 and October 2020. Means ± 1 standard deviation were shown.

Posotion	P_f (g m^{-2} y^{-1})	ΔB_f (g m^{-2} y^{-1})	M_f (g m^{-2} y^{-1})	Mean B_f (g m^{-2})	Turnover rate (y^{-1})	Mean B_c (g DMm^{-2})
Near	115 ± 20	3 ± 48	112 ± 98	133 ± 40	0.90 ± 0.31	44 ± 42
Far	102 ± 29	4 ± 26	98 ± 33	78 ± 43	1.67 ± 0.89	20 ± 26

3.2.4. Sap flow

Sap flow rates (T_r) normalized by fine root biomass were measured form July of 2019 to November of 2020 with a suspension of five months in the leafless season. Daily T_r showed a similar seasonal variation with that of Ts (Fig. 3.19). During the leafless season between November and April, T_r would have been zero.

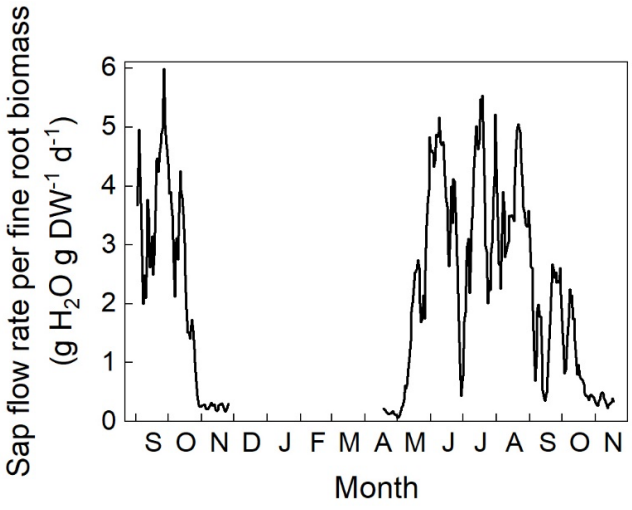

Fig. 3.19. Daily sap flow rates per fine root biomass (T_r). Mean of five-day moving average is shown (n = 3)

3.2.5. Partitioning root respiration

Model 1 (Eq. 6) and Model 2 (Eq. 7) were significantly fitted to the data set ($p < 0.001$) with an adjusted r^2 of 0.51 and 0.53, respectively (Table 3.11). All parameters were also significantly determined ($p < 0.05$). The parameters related to R_m (d and f) were almost the same for the models. The Q_{10} derived from f was 2.46–2.61. However, the parameter related to R_g (c) was smaller in Model 2 by 18%; the difference was due to adding R_{ion}. Part of R_g was distributed into R_{ion}.

We partitioned R_r using Model 2, because r^2 was slightly larger in Model 2 (Table 3.12). Annually, qt Near, R_g of fine roots, R_m of fine roots, R_{ion} and R_m of coarse roots accounted for 27, 48, 10 and 15% of their sum (estimated R_r), respectively. The bias between R_r from Table 3.8 and the estimated R_r was 5 g C m^{-2} yr^{-1} (2%). Meanwhile, R_g of fine roots, R_m of fine roots, R_{ion} and R_m of coarse roots accounted for 37, 43, 9 and 12% of their sum at Far; the bias was 35 g C m^{-2} yr^{-1} (20%). The respirations were spatially averaged with a weight of circumference: 3.14 and 6.28 m for Near and Far, respectively. As a result, R_g of fine roots, R_m of fine roots, R_{ion} and R_m of coarse roots accounted for 32, 46, 9 and 13% of the total R_r on average in a circumferential area between 0.5 and 1.0 m in radius.

The R_g varied seasonally in parallel with P_f (Fig. 3.16), whereas R_m varied mainly according to a seasonal variation in T_s (Fig. 3.10a). Thus, R_g peaked earlier than R_m.

Table 3.11. Fitting parameters of Eqs. 6 and 7 (n = 144) (± 1 standard error) with significance (p value).

	Model 1 (Eq. 6)		Model 2 (Eq. 7)	
	Parameter	p-value	Parameter	p-value
c (g C g DM^{-1})	0.73 ± 0.13	< 0.001	0.60 ± 0.14	< 0.001
d (g C g DM^{-1} d^{-1})	0.00081 ± 0.00025	0.001	0.00080 ± 0.00026	0.002
f (°C^{-1})	0.096 ± 0.014	< 0.001	0.090 ± 0.015	< 0.001
g (g C g H_2O^{-1})			0.00039 ± 0.00018	0.033
Adjusted r^2	0.51		0.53	
p-value	< 0.001		< 0.001	

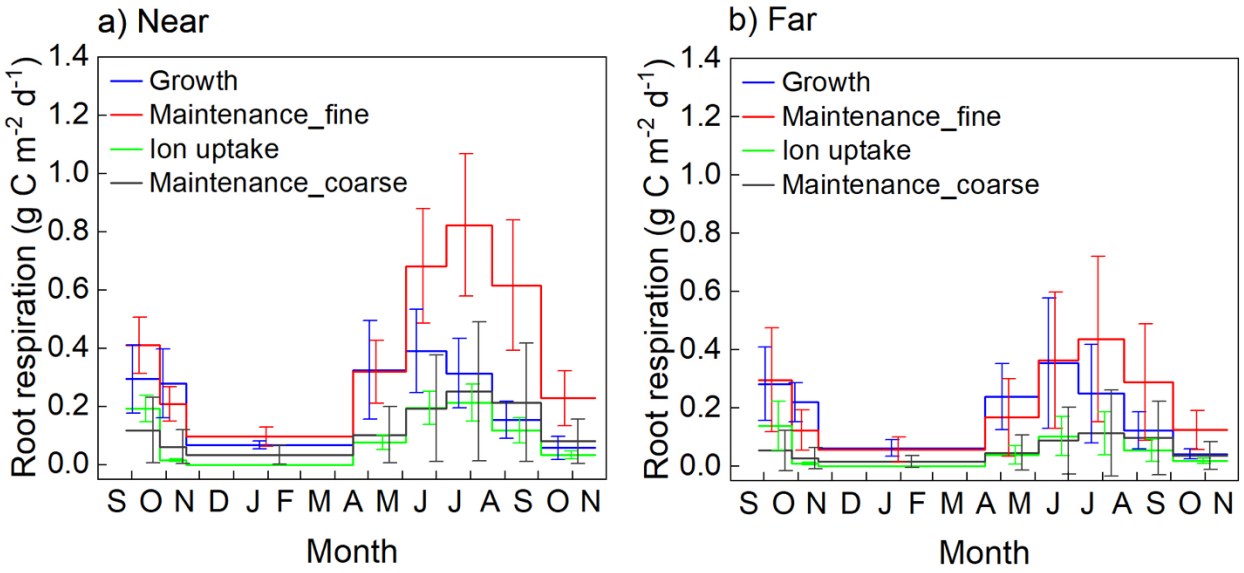

Fig. 3. 20. Seasonal variations of fine root growth respiration (R_g), fine root maintenance respiration (R_{m_fine}), ion uptake respiration (R_{ion}) and coarse root maintenance respiration (R_{m_coarse}) at Near and Far (n = 9) calculated using Model 2 between September 2019 and November 2020. Means ± 1 standard deviation are shown

Table 3.12. Annual sums (g C m^{-2} yr^{-1}) of root respiration (R_r) from Table 3.8, fine root growth respiration (R_g), fine root maintenance respiration (R_{m_fine}), ion uptake respiration (R_{ion}), coarse root maintenance respiration (R_{m_coarse}) and the sum of R_g, R_{m_fine}, R_{ion} and R_{m_coarse} (Sum) at Near and Far (n = 9), which corresponds to R_r. Values at Near and Far were spatially averaged with a weight of circumference: 6.28 and 9.42 m for Near and Far, respectively (weighted average). Means ±1 standard deviation are shown. Numbers in parentheses denote percentages against Sum.

Position	R_r	R_g	R_{m_fine}	R_{ion}	R_{m_coarse}	Sum
Near	287 ± 86 (98)	78 ± 16 (27)	141 ± 41 (48)	28 ± 8 (10)	45 ± 43 (15)	292 ± 73 (100)
Far	212 ± 104 (120)	65 ± 18 (37)	76 ± 49 (43)	15 ± 10 (9)	21 ± 26 (12)	177 ± 97 (100)
Weighted average	237 (110)	69 (32)	98 (46)	19 (9)	29 (13)	215 (100)

4. Discussion

In the previous study conducted in the same area (Sun *et al.*, 2020), fine root dynamics and soil CO_2 efflux were measured simultaneously within the same collar over a year in adjacent larch-dominated deciduous (DF) and evergreen conifer (EF) forests, annual R_g and R_m of tree fine roots were quantified on an annual basis using a multiple regression model. However, the results would include considerable uncertainty because of relatively complex experimental conditions in the field, which arose from forest maturity and rich understory species. The mature forests were relatively rich in SOM, litter accumulation and roots. Thus, the forests had a large spatial variation in R_h originating from SOM and litter accumulation. The large spatial variation made it difficult to separate R_s into R_h and R_r in each pair of collars, because R_h was not presumed to be identical even in two neighboring collars. Consequently, representative R_r was determined from the averages of R_s and R_h in each forest, resulting in a small number of available data for curve fitting (n = 5). In addition, the DF had canopy gaps caused by a windstorm, and consequently was rich in herbaceous plants. Thus, in the mature forests, a good portion of R_r originated from coarse roots and herbaceous roots, not fine roots targeted for the study.

In this study, we conducted a similar field experiment over a year twice in a larch-dominated young forest developing on the bare ground after removing surface organic soil along with coarse woody debris to obtain robust results by simplifying experimental conditions and improving the model. The study site was poor in SOM and litter accumulation. Soil C concentration was about 30% of that in DF and showed a decreasing tendency with a distance from tree stems, which was probably caused by the gradient of litter fall. Thus, we believe that R_h was almost equal in each pair by setting two collars on a concentric fashion from an isolated larch tree, which was supported by the fact that R_s was not significantly different in each pair before trenching (Fig. 3.2). Coefficients of variance (CV) in annual R_h were 24% (Near) and 30% (Far) in Experiment 1 (Table 3.8) and 23% (Near) and 27% (Far) in Experiment 2 (Table 3.2), which were much smaller than those of DF (59%) and EF (39%). The small CV also supported the smaller spatial variation in R_h. As a result, we were able to calculate R_r in each

pair and prepare 50 and 144 data sets in total for curve fitting, respectively, in Experiment 1 and 2. By separating positions into Near (0.5 m) and Far (1.0 m), we were able to use a wide range of data and make significant fitting (Tables 3.4 and 3.11). In addition, understory vegetation was very scarce, and the density of coarse roots (≥ 2 mm) was low with 44 ± 42 and 20 ± 26 g m^{-2}, respectively, at Near and Far in Experiment 2 (Table 3.9). The contribution of fine roots to total R_r was large at 83–85% at Near (Tables 3.5 and 3.12), whereas it was 45% and 68%, respectively, at DF and EF. In Sun *et al*. (2020), the large R_r of coarse roots and herbaceous roots (55 and 32%) were treated as a residual without seasonality. In this study, we related coarse root biomass (B_c) with T_s to estimate R_m. Since root density was low (Tables 3.3 and 3.9), annual CO_2 emissions through dead root decomposition (R_{DR}) was also small at 13 (Near) and 8 (Far) g C m^{-2} yr^{-1} in Experiment 1 (Table 3.2) and 33 (Near) and 20 (Far) g C m^{-2} yr^{-1} in Experiment 2 (Table 3.8), which accounted only 3–5% of R_s. The small R_{DR} contributed to decrease uncertainty in estimating R_h (= $R_{TC} - R_{DR}$) and consequently R_r. Moreover, although trenching decreases SWC owing to lack of water uptake by roots (Subke *et al*., 2006; Sun *et al*. 2020), no significant SWC decrease was found in trenched collars in Experiment 1 (Table 3.1). In contrast, SWC was significantly higher in trenched collars in Experiment 2 (Table 3.6). Anyway, the difference was small and the effect of SWC change would be negligible (Fig. 3.12).

We improved the reliability of partitioning fine root respiration, as described above. However, there is still uncertainty. Although the temperature response of coarse root R_m was incorporated into the model on the assumption that the temperature coefficient (*f*) was the same as that of fine root R_m, seasonal variation in B_c was not considered using a fixed B_c measured after Experiment 2. The R_g of coarse roots was also ignored, whereas an annual tree survey using allometric equations suggested an annual coarse root growth of 76 g m^{-2} yr^{-1} bewteen 2017 and 2018. The B_c was calculated to be 276 g m^{-2} in 2017 and 352 g m^{-2} in 2018 for larch trees, accounting for 79% of all coarse root biomass. In this study, B_c was 55 and 49 g m^{-2}, respectively, at Near and Far in Experiment 1, which were only 14–20% of the tree survey result. The reasons for the small B_c are that biomass within 0.5 m from trees was not included, and that soil samples were taken round isolated larch trees. Wieser and Bahn (2004)

continuously measured the coarse root R_r of *Pinus cembra* and reported that R_m accounted for 73–80% of the sum of R_m and R_g. Using the percentage, the R_g of coarse roots was roughly estimated from coarse root R_m to be 6–8 and 5–7 g m^{-2} yr^{-1}, respectively, at Near and Far, which accounted for about 15% (Near) and 25% (Far) of fine root R_g in Experiment 1 (Table 3.5). In addition, we did not directly measure ion uptake, mainly consisting of nitrogen uptake. Instead, we used water uptake by roots estimated from daily sap flow rates. It is reported that R_{ion} is proportional to water uptake in the condition of low root density, such as in our study site (Oyewole et al., 2014; Henriksson et al., 2021). Also, R_{ion} is expected to correlate with photosynthesis (Lambers *et al*., 2008), and fine roots are mainly produced using recent photosynthate (Lynch *et al*., 2013). Moreover, it is reported that gross primally production (GPP) is proportional to transpiration rates on a monthly basis (Scott and Biederman, 2017). Thus, sap flow rates would be proportional to ion uptake.

Since the study site was a young forest with a small amount of soil carbon, litter accumulation and roots, soil CO_2 efflux was considerably smaller than those of adjacent forests. For example, annual values of P_f, mortality (M_f) and mean B_f at Near were 22, 26 and 30% of those in DF, respectively, in Experiment 1 (Table 3.3). As a result, annual R_s and R_r at Near was 39 and 29% of those in DF (Table 3.2). In contrast, annual R_h at Near accounted for 74% of that in DF, even though soil carbon concentration was only 30% of that in DF. The larger R_h than expected from carbon concentration was probably due to a difference in the decomposability of SOM. Older SOM in DF could have more recalcitrant fractions (Ryan and Law, 2005). The growth respiration coefficient (g_R) of 0.60 g C g DM^{-1} (Model 2 in Experiment 2) is equivalent to 50 mmol CO_2 g DM^{-1} and almost doubles those in DF and EF (Table 3.11). Meanwhile, the maintenance respiration coefficients (g_m), which is equivalent to $d \cdot \exp(f \cdot T_s)$, were 1.3, 3.1 and 7.6 nmol CO_2 g DM^{-1} s^{-1} at 5, 15 and 25°C, respectively (Model 2 in Experiment 2). Although the g_m at 25°C was equal to that in DF, g_m was 1.2 and 1.7 times higher at 5 and 15°C, respectively, because the base coefficient (d) was higher but the temperature coefficient (f) was lower than those in DF. In comparison with previous studies conducted in the field for *Pinus taeda* and *Liquidambar styaciflua* (George *et al*., 2003) and in a greenhouse for eucalyptus cuttings (Thongo M'Bou *et al*., 2010), the g_R and g_m of this study

were about ten times higher and slightly lower, respectively. The variation in the coefficients is mainly due to differences in species, environmental conditions and methods (Lambers *et al*., 2008).

The Q_{10} values calculated from a seasonal variation in soil CO_2 efflux was reported to be higher in R_r than in R_h (Boone *et al*., 1998; Wang *et al*., 2010), because it is confounded with root phenology like in Figs. 3.6 and 3.7. Wang *et al*. (2010) also reported that the mean Q_{10} values from 13 forest sites were 3.40 and 2.42, respectively, for R_r and R_h. In this study, the Q_{10} of R_r was about 2.0 and was equivalent to that of R_h. We think that the lower Q_{10} of 2.0 was quite possible, because it was a combined result of the apparent Q_{10} values of P_f (4.48 and 2.51), B_f (1.08 and 1.49) (Fig. 3.7) and R_m. However, uncertainty might be large in Q_{10} calculation, because CO_2 efflux data at low temperatures were insufficient; Q_{10} is sensitive to data at low temperatures.

Soil CO_2 efflux was continuously estimated from the monitoring data of T_s (Figs. 3.1a and 3.10a) using an exponential equation (Eq. 2). Although constant R_s of 0.61 and 0.42 g C m^{-2} d^{-1} in experiment 1 were shown during the snowy season in Fig. 3.5, the R_s might be a little overestimated in comparison with winter R_s (0.5 g C m^{-2} d^{-1}) measured under snow in an undisturbed deciduous forest about 5 km apart from the study site (Hirano, 2005). The overestimation was probable caused by uncertainty of the parameters of Eq. 2 (Fig. 3.3), because data were lacking at low temperatures (< 10°C). In the dormant season, roots respire using NSC accumulated during the previous growing season (Furze *et al*., 2019; Collalti *et al*., 2020). Small P_f of about 0.04 g m^{-2} d^{-1} was measured both at Near and Far in the cold season from mid-November to mid-May in Experiment 1 (Fig. 3.6b). Although some studies reported fine root growth in winter (Radville *et al*., 2016), the P_f might include spring P_f after snowmelt in early April. The fine root R_g, R_m and R_{ion} showed obvious seasonal variations (Figs. 3.9 and 3.20), reflecting the seasonality of P_f, T_s and T_r, respectively. At Near, R_g was smaller than R_m throughout a year (Figs. 3.9c and 3.20).

5. Conclusions

In comparison with the previous study conducted in the same area, we incorporated the maintenance respiration of coarse roots and ion uptake respiration in the model for partitioning of root respiration. Moreover, we simplified the experimental conditions in the field and controlled spatial variation in heterotrophic respiration and contamination from roots other than fine roots. The improvement decreased uncertainty in experiments and considerably increased data size available for model parametrization. As a result, we succeeded in significant partitioning of root respiration into fine root growth respiration, fine root maintenance respiration, ion uptake respiration and coarse root maintenance respiration from root dynamics and sap flow rates. Also, we quantified the seasonal variation of the growth, maintenance and ion uptake respirations, along with fine root dynamics. To improve the partitioning further, spatial variation in coarse root density should be considered, and more frequent measurement of fine root dynamics is given priority.

Acknowledgment

First and foremost, I would like to express my sincere and deep gratitude to my advisor and mentor, Prof. Takashi Hirano. Without his continuous support and patient guidance throughout the entire journey of my PhD, this thesis would have never been accomplished. Apart from the learning experience of mine, life at Hokkaido University was so much easier with his constant kindness and warm support. Not only being an academic mentor, he is a moral model whom I will continue to respect and emulate for the rest of my life. What I have learned from him will keep inspiring me in the future.

I would also like to acknowledge my senior Dr. Lifei Sun for his generous assistance. He carefully demonstrated and expertly pointed many mistakes and deadlocks I have made and has saved me from taking the wrong routes in my study. When I first arrived in Japan as an international student, his help meant everything to me during difficult times.

Special thanks to Dr. Naishen Liang and Dr. Munemas Teramoto for instrumentation and sampling analysis for my research. Although we only met a few times, I could always be touched by their passion for research, and it deeply motivated me.

I would also like to extend my deepest appreciation to Prof. Ryoji Sameshima and Prof. Tomomichi Kato as the examiner of my thesis. They shared their valuable knowledge and offered much advice on my work.

It is my pleasure and fortune to thank the Hokkaido Regional Office of the Forestry Agency for allowing me to use their study site. I acknowledge the support of JPSP KAKENHI and the Environment Research and Technology Development Fund of Environmental Restoration and Conservation Agency of Japan. I humbly give my gratitude to the Government of Japan through the Japan Student Services Organization for the scholarship (The Monbukagakusho Honors Scholarship for Privately-Financed International Students).

To all members of the laboratory of Environmental and Ecological Physics, thank you for all the encouragement, care, and delight. The time spent with you is a fantastic, unforgettable, and priceless experience to me.

Last but not least, I would like to convey my thanks to my family and friends, whose mental endorsement help me go through the epidemic. I will be forever grateful for your love.

References

Abramoff, R. Z., and A. C. Finzi. 2015. 'Are above- and below-ground phenology in sync?', *New Phytol*, 205: 1054-61.

Amthor, J. 2000. 'The McCree–de Wit–Penning de Vries–Thornley Respiration Paradigms: 30 Years Later', *Annals of Botany*, 86: 1-20.

Beer, C., M. Reichstein, E. Tomelleri, P. Ciais, M. Jung, N. Carvalhais, C. Rodenbeck, M. A. Arain, D. Baldocchi, G. B. Bonan, A. Bondeau, A. Cescatti, G. Lasslop, A. Lindroth, M. Lomas, S. Luyssaert, H. Margolis, K. W. Oleson, O. Roupsard, E. Veenendaal, N. Viovy, C. Williams, F. I. Woodward, and D. Papale. 2010. 'Terrestrial gross carbon dioxide uptake: global distribution and covariation with climate', *Science*, 329: 834-8.

Bond-Lamberty, B., and A. Thomson. 2010. 'Temperature-associated increases in the global soil respiration record', *Nature*, 464: 579-82.

Boone, R. D., K. J. Nadelhoffer, J. D. Canary, and J. P. Kaye. 1998. 'Roots exert a strong influence on the temperature sensitivity of soil respiration', *Nature*, 396: 570-72.

Brunner, I., M. R. Bakker, R. G. Björk, Y. Hirano, M. Lukac, X. Aranda, I. Børja, T. D. Eldhuset, H. S. Helmisaari, C. Jourdan, B. Konôpka, B. C. López, C. Miguel Pérez, H. Persson, and I. Ostonen. 2013. 'Fine-root turnover rates of European forests revisited: an analysis of data from sequential coring and ingrowth cores', *Plant and Soil*, 362: 357-72.

Cannell, M. G. R., and J. H. M. Thornley. 2000. 'Modeling the components of plant respiration: some guiding principle', *Annals of Botany*, 85: 45-54.

Chapin, F. S. III, P. A. Matson, and P. M Vitousek. 2011. 'Plant carbon buddgets.' in, *Principle of terrestrial ecosystem eclogoy* (Springer: New York).

Chen, Dima, Yang Zhang, Yongbiao Lin, Hua Chen, and Shenglei Fu. 2009. 'Stand level estimation of root respiration for two subtropical plantations based on in situ measurement of specific root respiration', *Forest Ecology and Management*, 257: 2088-97.

Collalti, A., M. G. Tjoelker, G. Hoch, A. Makela, G. Guidolotti, M. Heskel, G. Petit, M. G. Ryan, G. Battipaglia, G. Matteucci, and I. C. Prentice. 2020. 'Plant respiration: Controlled by photosynthesis or biomass?', *Glob Chang Biol*, 26: 1739-53.

Davidson, E. A., A. D. Richardson, K. E. Savage, and D. Y. Hollinger. 2006. 'A distinct seasonal pattern of the ratio of soil respiration to total ecosystem respiration in a spruce-dominated

forest', *Global Change Biology*, 12: 230-39.

Epron, D. 2009. 'Separating autotrophic and heterotrophic components of soil respiration: lessons learned from trenching and related root-exclusiong experiments.' in W. Kutsch, M. Bahn and Andreas Heinemeyer (eds.), *Soil Carbon Dynamics* (Cambridge University Press: New York).

Finér, Leena, Mizue Ohashi, Kyotaro Noguchi, and Yasuhiro Hirano. 2011. 'Fine root production and turnover in forest ecosystems in relation to stand and environmental characteristics', Forest Ecology and Management, 262: 2008-23.

Fukuzawa K, Shibata H, Takagi K, Satoh F, Koike T, Sasa K. 2013. 'Temporal variation in fine-root biomass, production and mortality in a cool temperate forest covered with dense understory vegetation in northern Japan.', *Forest Ecol Manag* 310:700–710.

Furze, M. E., B. A. Huggett, D. M. Aubrecht, C. D. Stolz, M. S. Carbone, and A. D. Richardson. 2019. 'Whole-tree nonstructural carbohydrate storage and seasonal dynamics in five temperate species', *New Phytol*, 221: 1466-77.

George, K., R. J. Norby, J. G. Hamilton, and E. H. DeLucia. 2003. 'Fine-root respiration in a loblolly pine and sweetgum forest growing in elevated CO2', *New Phytologist*, 160: 511-22.

Gholz, H. L., D. A. Wedin, S. M. Smitherman, M. E. Harmon, and W. J Parton. 2000. 'Long-term dynamics of pine and harwood litter in contrasting environments: towards a global model of decomposition', Global Change Biology, 6: 751-65.

Granier, André. 1987. 'Evaluation of transpiration in a Douglas-fir stand by means of sap flow measurements.' *Tree physiology*, 3: 309-320.

Hanson, P. J., N. T. Edwards, C. T. Gartedn, and J. A. Andrews. 2000. 'Separating root and soil microbial contributions to soil respiration: A review of methods and observations', *Biogeochemistry*, 48: 114-46.

Hirano, T. 2005. 'Seasonal and diurnal variations in topsoil and subsoil respiration under snowpack in a temperate deciduous forest', *Global Biogeochemical Cycles*, 19.

Hirano, T, R Hirata, Y Fujinuma, N Saigusa, S Yamamoto, Y Harazono, M Takada, K Inukai, and G Inoue. 2003. 'CO2 and water vapor exchange of a larch forest in northern Japan', *Tellus Series B-Chemical and Physical Meteorology*, 55: 244-57.

Hirano, T., K. Suzuki, and R. Hirata. 2017. 'Energy balance and evapotranspiration changes in a larch forest caused by severe disturbance during an early secondary succession', *Agricultural and Forest Meteorology*, 232: 457-68.

Hirata, Ryuichi, Takashi Hirano, Nobuko Saigusa, Yasumi Fujinuma, Koh Inukai, Yasuyuki Kitamori, Yoshiyuki Takahashi, and Susumu Yamamoto. 2007. 'Seasonal and interannual variations in carbon dioxide exchange of a temperate larch forest', *Agricultural and Forest Meteorology*, 147: 110-24.

Janssens IA, Lankreijer H, Matteucci G, Kowalski AS, Buchmann N, Epron D, Pilegaard K, Kutsch W, Longdoz B, Grunwald T, Montagnani L, Dore S, Rebmann C, Moors EJ, Grelle A, Rannik U, Morgenstern K, Oltchev S, Clement R, Gudmundsson J, Minerbi S, Berbigier P, Ibrom A, Moncrieff J, Aubinet M, Bernhofer C, Jensen NO, Vesala T, Granier A, Schulze ED, Lindroth A, Dolman AJ, Jarvis PG, Ceulemans R, Valentini R. 2001. 'Productivity over- shadows temperature in determining soil and ecosystem res- piration across European forests.', *Glob Chang Biol* 7:269– 278.

Johnson, I. R. 1990. 'Plant respiration in relation to growth, maintenance, ion uptake and nitrogen assimilation', *Plant, Cell and Environment*, 13: 319-28.

Lambers, H., F. S. III Chapin, and T. L. Pons. 2008. 'The role of respiration in plant carbon balance.' in, *Plant Physiological Ecology* (Springer: New York).

Lavigne, M. B., R. J. Foster, and G. Goodine. 2004. 'Seasonal and annual changes in soil respiration in relation to soil temperature, water potential and trenching', *Tree Physiology*, 24: 415-24.

Lynch, D. J., R. Matamala, C. M. Iversen, R. J. Norby, and M. A. Gonzalez-Meler. 2013. 'Stored carbon partly fuels fine-root respiration but is not used for production of new fine roots', *New Phytol*, 199: 420-30.

Makita, N., Y. Kosugi, M. Dannoura, S. Takanashi, K. Niiyama, A. R. Kassim, and A. R. Nik. 2012. 'Patterns of root respiration rates and morphological traits in 13 tree species in a tropical forest', Tree Physiol, 32: 303-12.

Makkonen K, Helmisaari HS. 1998. 'Seasonal and yearly varia- tions of fine-root biomass and necromass in a scots pine (Pinus sylvestris L.) stand.', *Forest Ecol Manag* 102:283–290

Marsden, C., Y. Nouvellon, A. T. M'Bou, L. Saint-Andre, C. Jourdan, A. Kinana, and D. Epron.

2008. 'Two independent estimations of stand-level root respiration on clonal Eucalyptus stands in Congo: up scaling of direct measurements on roots versus the trenched-plot technique', *New Phytol*, 177: 676-87.

McCormack, M. L., I. A. Dickie, D. M. Eissenstat, T. J. Fahey, C. W. Fernandez, D. Guo, H. S. Helmisaari, E. A. Hobbie, C. M. Iversen, R. B. Jackson, J. Leppalammi-Kujansuu, R. J. Norby, R. P. Phillips, K. S. Pregitzer, S. G. Pritchard, B. Rewald, and M. Zadworny. 2015. 'Redefining fine roots improves understanding of below-ground contributions to terrestrial biosphere processes', *New Phytol*, 207: 505-18.

McCree, K. J. 1974. 'Equation for the rae of dark respiration of white clove and grain sorghum, as functions of dry weight, photosynthetic rate, and tempearture', *Crop Science*, 14: 509-14.

Moyano, Fernando E., Owen K. Atkin, M. Bahn, Dan Bruhn, Andrew J. Burton, Andreas Heinemeyer, Werner L. Kutsch, and Gerhard Wieser. 2009. 'Respiration from roots and the mycorrhizosphere.' in Werner L. Kutsch, M. Bahn and Andreas Heinemeyer (eds.), *Soil Carbon Dynamics* (Cambridge University Press: New York).

Neumann, M., D. L. Godbold, Y. Hirano, and L. Finer. 2020. 'Improving models of fine root carbon stocks and fluxes in European forests', Journal of Ecology, 108: 496-514.

Noguchi K, Sakata T, Mizoguchi T, Takahashi M. 2005. 'Estimating the production and mortality of fine roots in a Japanese cedar (Cryptomeria japonica D. Don) plantation using a minirhizotron technique.', *J Forest Res-Jpn* 10:435– 441.

Penning de Vries, F. W. T. 1974. 'Substrate utilization and respiration in relation to growth and maintenance in higher plants', *Netherlands Journal of Agricultural Science*, 22: 40-44.

Radville, L., M. L. McCormack, E. Post, and D. M. Eissenstat. 2016. 'Root phenology in a changing climate', *J Exp Bot*, 67: 3617-28.

Rewald, B., A. Rechenmacher, and D. L. Godbold. 2014. 'It's complicated: intraroot system variability of respiration and morphological traits in four deciduous tree species', *Plant Physiol*, 166: 736-45.

Richter, Daniel D., Daniel Markewitz, S. E. Trumbore, and Carol G. Wells. 1999. 'Rapid accumulation and turnover of soil carbon in a re-establishing forest', *Nature*, 400: 56-58.

Ryan, M. G., and B. E. Law. 2005. 'Interpreting, measuring, and modeling soil respiration',

Biogeochemistry, 73: 3-27.

Sano, Tomohito, Takashi Hirano, Naishen Liang, Ryuichi Hirata, and Yasumi Fujinuma. 2010. 'Carbon dioxide exchange of a larch forest after a typhoon disturbance', *Forest Ecology and Management*, 260: 2214-23.

Scott-Denton, Laura E., Todd N. Rosenstiel, and Russell K. Monson. 2006. 'Differential controls by climate and substrate over the heterotrophic and rhizospheric components of soil respiration', *Global Change Biology*, 12: 205-16.

Silver, W. L., and R. K. Miya. 2001. 'Global patterns in root decomposition: comparisons of climate and litter quality effects', *Oecologia*, 129: 407-19.

Subke, Jens-Arne, Ilaria Inglima, and M. Francesca Cotrufo. 2006. 'Trends and methodological impacts in soil CO2 efflux partitioning: A metaanalytical review', *Global Change Biology*, 12: 921-43.

Sun, L. F., M. Teramoto, N. Liang, T. Yazaki, and T. Hirano. 2017. 'Comparison of litter-bag and chamber methods for measuring CO2 emissions from leaf litter decomposition in a temperate forest', *Journal of Agricultural Meteorology*, 73: 59-67.

Sun, Lifei, Takashi Hirano, Tomotsugu Yazaki, Munemasa Teramoto, and Naishen Liang. 2020. 'Fine root dynamics and partitioning of root respiration into growth and maintenance components in cool temperate deciduous and evergreen forests', *Plant and Soil*, 446: 471-86.

Sun, Qingling, Baolin Li, Tao Zhang, Yecheng Yuan, Xizhang Gao, Jinsong Ge, Fei Li, and Zhijun Zhang. 2017. 'An improved Biome-BGC model for estimating net primary productivity of alpine meadow on the Qinghai-Tibet Plateau', *Ecological Modelling*, 350: 55-68.

Sweetlove, L. J., T. C. Williams, C. Y. Cheung, and R. G. Ratcliffe. 2013. 'Modelling metabolic CO(2) evolution--a fresh perspective on respiration', *Plant Cell Environ*, 36: 1631-40.

Thongo M'Bou, Armel, Laurent Saint-André, Agnès de Grandcourt, Yann Nouvellon, Christophe Jourdan, Fidèle Mialoundama, and Daniel Epron. 2010. 'Growth and maintenance respiration of roots of clonal Eucalyptus cuttings: scaling to stand-level', *Plant and Soil*, 332: 41-53.

Thornley, J. H. 2011. 'Plant growth and respiration re-visited: maintenance respiration defined

- it is an emergent property of, not a separate process within, the system - and why the respiration : photosynthesis ratio is conservative', *Ann Bot*, 108: 1365-80.

Thornley, J. H. M. 1970. 'Respiration, growth and maintenance in plants', *Nature*, 227: 304-05.

Vogt, K. A., D. J. Vogt, and J. Bloomfield. 1998. 'Analysis of some direct and indirect methods for estimating root biomass and production of forests at an ecosystem level', *Plant and Soil*, 200: 71-89.

Wieder, R. Kelman, and G. E. Lang. 1982. 'A critique of the analytical methods used in examining decomposition data obtained from litter bags', *Ecology*, 63: 1636-42.

Wieser, Gerhard, and Michael Bahn. 2004. 'Seasonal and spatial variation of woody tissue respiration in a Pinus cembra tree at the alpine timberline in the central Austrian Alps', *Trees*, 18.

Yuan, Z. Y., and H. Y. Chen. 2012. 'Indirect methods produce higher estimates of fine root production and turnover rates than direct methods', *PLoS ONE*, 7: e48989.

Yuan, Z. Y., and Han Y. H. Chen. 2010. 'Fine Root Biomass, Production, Turnover Rates, and Nutrient Contents in Boreal Forest Ecosystems in Relation to Species, Climate, Fertility, and Stand Age: Literature Review and Meta-Analyses', *Critical Reviews in Plant Sciences*, 29: 204-21.